

An Assessment of the Mechanistic Differences Between Two Integrin $\alpha_4\beta_1$ Inhibitors, the Monoclonal Antibody TA-2 and the Small Molecule BIO5192, in Rat Experimental Autoimmune Encephalomyelitis

D. R. LEONE, K. GIZA, A. GILL, B. M. DOLINSKI, W. YANG, S. PERPER, D. M. SCOTT, W.-C. LEE, M. CORNEBISE, K. WORTHAM, C. NICKERSON-NUTTER,¹ L. L. CHEN, D. LEPAGE, J. C. SPELL,² E. T. WHALLEY, R. C. PETTER, S. P. ADAMS,³ R. R. LOBB, and R. B. PEPINSKY

Biogen, Inc., Cambridge, Massachusetts

Received December 6, 2002; accepted March 5, 2003

ABSTRACT

Integrin $\alpha_4\beta_1$ plays an important role in inflammatory processes by regulating the migration of lymphocytes into inflamed tissues. Here we evaluated the biochemical, pharmacological, and pharmacodynamic properties and efficacy in experimental autoimmune encephalomyelitis (EAE), a model of multiple sclerosis, of two types of $\alpha_4\beta_1$ inhibitors, the anti-rat α_4 monoclonal antibody TA-2 and the small molecule inhibitor BIO5192 [2(S)-[1-(3,5-dichloro-benzenesulfonyl)-pyrrolidine-2(S)-carbonyl]-amino]-4-[4-methyl-2(S)-(methyl-{2-[4-(3-*o*-tolyl-ureido)-phenyl]-acetyl}-amino)-pentanoylamino]-butyric acid]. TA-2 has been extensively studied in rats and provides a benchmark for assessing function. BIO5192 is a highly selective and potent (K_D of <10 pM) inhibitor of $\alpha_4\beta_1$. Dosing regimens were identified for both inhibitors, which provided full receptor occupancy during the duration of the study.

Both inhibitors induced leukocytosis, an effect that was used as a pharmacodynamic marker of activity, and both were efficacious in the EAE model. Treatment with TA-2 caused a decrease in α_4 integrin expression on the cell surface, which resulted from internalization of α_4 integrin/TA-2 complexes. In contrast, BIO5192 did not modulate cell surface $\alpha_4\beta_1$. Our results with BIO5192 indicate that $\alpha_4\beta_7$ does not play a role in this model and that blockade of $\alpha_4\beta_1$ /ligand interactions without down-modulation is sufficient for efficacy in rat EAE. BIO5192 is highly selective and binds with high affinity to $\alpha_4\beta_1$ from four of four species tested. These studies demonstrate that BIO5192, a novel, potent, and selective inhibitor of $\alpha_4\beta_1$ integrin, will be a valuable reagent for assessing $\alpha_4\beta_1$ biology and may provide a new therapeutic for treatment of human inflammatory diseases.

Integrins are a large family of cell surface receptors that mediate cell/cell and cell/matrix interactions and signal transduction. They exist as noncovalent $\alpha\beta$ heterodimers of different combinations of α and β chains and share extensive structural homology. The leukocyte integrin $\alpha_4\beta_1$ regulates normal lymphocyte trafficking (Lobb and Hemler, 1994) and provides a key

costimulatory signal supporting cell activation (Clark and Brugge, 1995). During inflammatory responses, it regulates lymphocyte migration into the damaged tissues and thus has been recognized as an attractive therapeutic target. In vivo studies using blocking monoclonal antibodies (Lobb and Hemler, 1994) and inhibitory peptides (Molossi et al., 1995) have verified the critical role of $\alpha_4\beta_1$ integrins in leukocyte-mediated inflammation. Numerous EAE models of multiple sclerosis have been designed to recapitulate important aspects of the disease and are responsive to α_4 inhibitors (Yednock et al., 1992). Recent positive phase II data using the anti- α_4 antibody

¹ Current address: Wyeth, Cambridge, MA.

² Current address: Bayer Corporation, West Haven, CT.

³ Current address: Neogenesis, Cambridge, MA.

Article, publication date, and citation information can be found at <http://jpet.aspetjournals.org>.

DOI: 10.1124/jpet.102.047332.

ABBREVIATIONS: EAE, experimental autoimmune encephalomyelitis; mAb, monoclonal antibody; LIBS, ligand-induced binding site; VCAM-1, vascular cell adhesion molecule-1; CS1, connecting segment 1; BIO1211, 4-((*N'*-2-methylphenyl)ureido)-phenylacetyl-leucine-aspartic acid-valine-proline; BIO7662, 2S-[1-(benzenesulfonyl-pyrrolidine-2S-carbonyl)-amino]-4-[4-methyl-2S-(methyl-{2-[4-(3-*o*-tolyl-ureido)-phenyl]-acetyl}-amino)-pentanoylamino]-butyric acid; HPLC, high pressure liquid chromatography; BSA, bovine serum albumin; PBS, phosphate-buffered saline; TBS, TRIS-buffered saline; FACS, fluorescence-activated cell sorter; FBS, fetal bovine serum; BOC, *t*-butoxycarbonyl; DMF, dimethyl formamide; HATU, *O*-(7-azabenzotriazol-1-yl)-*N,N,N',N'*-tetramethyluronium hexafluorophosphate; PBL, peripheral blood lymphocyte; PEG, polyethylene glycol; PE, phycoerythrin; NHS, *N*-hydroxysuccinimide; PK, pharmacokinetics; PD, pharmacodynamics; AUC, area under the curve; ELISA, enzyme-linked immunosorbent assay; MES, 2-(*N*-morpholino)ethanesulfonic acid; MBP, myelin basic protein; TNF, tumor necrosis factor; MAdCAM, mucosal addressin cell adhesion molecule; MS, mass spectroscopy.

natalizumab in patients with multiple sclerosis have validated $\alpha_4\beta_1$ as an important clinical target (Miller et al., 2003).

The anti-rat α_4 -chain monoclonal antibody, TA-2, has been used extensively to study the role of α_4 integrins in models of inflammatory disease. TA-2 blocked α_4 integrin-mediated lymphocyte migration to inflammatory sites and homing to lymphoid tissues (Issekutz, 1991; Issekutz and Wykretowicz, 1991). In studies of lung inflammation in the Brown Norway rat, TA-2 treatment blocked α_4 -expressing eosinophil and neutrophil migration into the pleural cavity and decreased late airway responses in ovalbumin-sensitized and challenged rats, suggesting a use in the treatment of asthma (Taylor et al., 1997; Hojo et al., 1998; Schneider et al., 1999; Ramos-Barbon et al., 2001). TA-2 was also used in Lewis rats to probe for α_4 /VCAM-1 (vascular cell adhesion molecule-1) interactions in experimental autoimmune neuritis, a model of Guillain-Barré syndrome, where it reduced disease severity and inflammation through a possible block of cell transmigration to the damaged nerve (Enders et al., 1998). A more recent study using TA-2 in this model suggested that at least part of the effect of the antibody was the result of induction of apoptosis of P2-specific T-cells (Leussink et al., 2002). Other studies demonstrated that TA-2 blocked blood polymorphonuclear cell migration to the inflamed joint even after joint inflammation had developed, proving that an anti- α_4 regimen is an effective arthritis treatment (Issekutz et al., 1996). It is not clear whether the mechanism of action of TA-2 is solely a consequence of its blocking α_4 /ligand interactions or other mechanisms or both. Although TA-2 is limited to studies in rats, other anti- α_4 mAbs have been used to further extend the list of potential uses for an inhibitor of $\alpha_4\beta_1$ (Lobb and Hemler, 1994). Because anti- α_4 antibodies block both $\alpha_4\beta_1$ and $\alpha_4\beta_7$, it is not possible to rule out involvement of $\alpha_4\beta_7$ in these studies.

$\alpha_4\beta_1$ mediates cell adhesion by binding to either of two protein ligands, VCAM-1, or the alternatively spliced connecting segment 1 (CS1)-containing fibronectin variant (Osborn et al., 1989; Wayner et al., 1989). More recently other potential ligands have been identified (Bayless et al., 1998; Takahashi et al., 2000); however, the biological significance of these interactions is less clear. The key residues in VCAM-1 (QIDSP) and CS1 (EILDVP) necessary for their interactions with $\alpha_4\beta_1$ have been defined by molecular and biochemical techniques (Wayner and Kovach, 1992; Wang et al., 1995). Many groups have used these sequences as starting points to develop small molecule inhibitors that can block the interaction between $\alpha_4\beta_1$ and its ligands (Abraham, 1997; Lin et al., 1999; Kudlacz et al., 2002; van der Laan et al., 2002). In studying the selectivity of different classes of $\alpha_4\beta_1$ inhibitors, we identified the small molecule inhibitor BIO5192 [2(S)-[1-(3,5-dichlorobenzenesulfonyl)-pyrrolidine-2(S)-carbonyl]-amino]-4-[4-methyl-2(S)-(methyl-[2-[4-(3-*o*-tolyl-ureido)-phenyl]-acetyl]-amino)pentanoylamino]-butyric acid] (D. M. Scott, manuscript in preparation). BIO5192 was of special interest because of its high affinity for $\alpha_4\beta_1$ under all states of activation, high selectivity for $\alpha_4\beta_1$, and slow dissociation rate from the bound complex. Here we compared and contrasted the biochemical, pharmacokinetic, and pharmacodynamic properties of BIO5192 and mAb TA-2, and demonstrate that both inhibitors effectively block the disease progression of EAE in rats. The clear distinction in the modes

of action of the two inhibitors has provided a means for better understanding the role of $\alpha_4\beta_1$ in EAE.

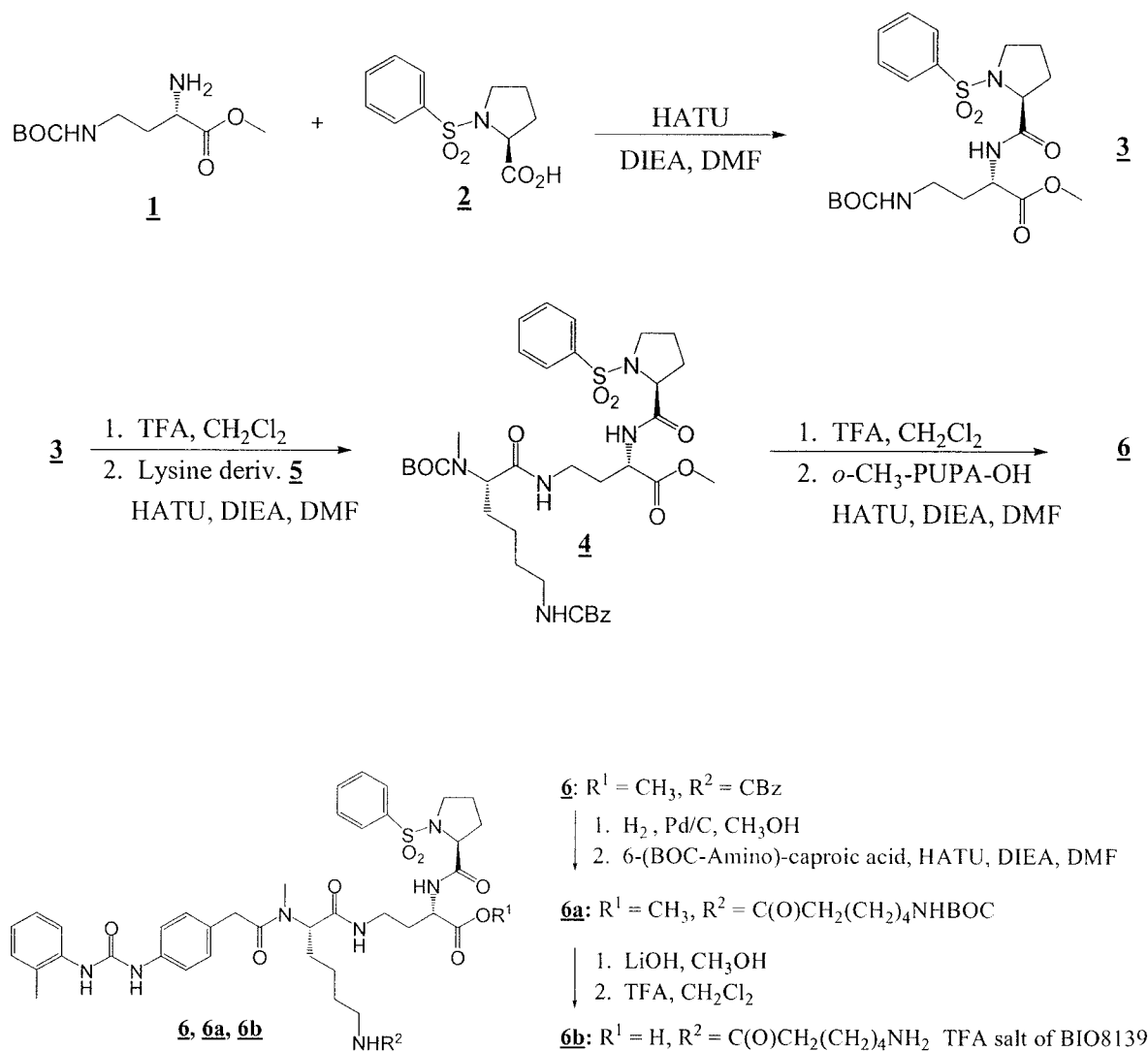
Materials and Methods

Cell Lines. The $\alpha_4\beta_1$ -expressing human T-cell line, Jurkat (a gift from S. Burakoff, Dana Farber Cancer Institute, Boston, MA) and the $\alpha_4\beta_7$ -expressing human B-cell line, JY, and the α_4 -expressing rat cell line, RBL.1 (American Type Tissue Collection, Manassas, VA) were maintained in culture at 37°C in RPMI-1640 medium and Earle's MEM, 1 mM sodium pyruvate, respectively, supplemented with 10% fetal bovine serum (FBS). K562 cell lines transfected with either the human α_9 integrin chain (Diane Leone, Biogen, Inc.) or with the human α_2 integrin chain (a gift from M. Hemler, Dana Farber Cancer Institute) were maintained in RPMI-1640 medium supplemented with 10% FBS and 1 mg/ml G418. An enriched population of the α_9 -K562 cells that exhibited high levels of $\alpha_9\beta_1$ expression was obtained by fluorescence-activated cell sorting (FACS), and this subclone was used for all subsequent work. All cells were periodically monitored for high integrin surface expression by FACS analysis (data not shown).

Synthesis of $\alpha_4\beta_1$ Small Molecule Inhibitors. BIO5192 was synthesized as previously described (D. M. Scott, manuscript in preparation). BIO8139, an amine-containing derivative of BIO5192 that was used for conjugation and the development of assays for assessing $\alpha_4\beta_1$ function, was prepared as follows (see Scheme below). SOCl_2 (14.6 ml, 200 mmol) was added dropwise over a period of 15 min to a suspension of 8.4 g (33.3 mmol) *N* α -CBZ-L-2,4-diaminobutyric acid in 200 ml of methanol at 0°C and stirred overnight at 23°C. The solution was concentrated and redissolved in methanol 3 times, then dissolved in CH_2Cl_2 , concentrated, and placed under high vacuum to give 10.33 g of the methyl ester. The crude ester was dissolved in 200 ml of CH_2Cl_2 and 16.2 ml (116.6 mmol) of triethylamine was added followed by 8.96 g (41 mmol) di-*tert*-butyl dicarbonate. After stirring at 23°C for 4 h, the solution was washed once with 1 N HCl, once with saturated NaHCO_3 solution, and once with saturated NaCl, then dried (Na_2SO_4), filtered, and concentrated to give a yellow syrup. Purification by flash column chromatography gave 9.6 g (26.3 mmol, 79%) of *t*-butoxycarbonyl (BOC) protected amine as a colorless syrup. Then 250 mg of 10% Pd/C was added to the solution of the BOC-protected amine in 100 ml of methanol and was stirred overnight under 60 psi of H_2 . The mixture was filtered through a plug of Celite and concentrated. 6.0 g (26 mmol, 78% yield) of compound **1** (*N* γ -Boc-L-2,4-diaminobutyric acid methyl ester) as a colorless oil was recovered, which was used without further purification. MS: m/z 232 ($\text{M} + \text{H}^+$).

Triethylamine (70 ml, 0.5 mol) was added to 25 g (0.15 mol) of L-proline methyl ester hydrochloride in 500 ml of CH_2Cl_2 . The resulting white precipitate was removed by filtration, and the filtrate was cooled to 0°C. 20 ml (0.15 mol) of benzenesulfonyl chloride in 50 ml of CH_2Cl_2 was added to the filtrate dropwise over a period of 15 min and stirred overnight at 23°C. The solution was washed with 1 N HCl, 1 NaOH, and saturated NaCl, then dried (MgSO_4), filtered, and concentrated to give a pale yellow solid. This material was recrystallized 3 times from ethyl acetate/hexane to give 38.2 g (0.142 mol, 95%) of *N*-(benzenesulfonyl)-proline methyl ester (thin layer chromatography versus 2:1 hexane/ethyl acetate, R_f = 0.35). The methyl ester was dissolved in 500 ml of methanol. 140 ml (0.28 mol) of freshly-prepared 2 M aqueous LiOH was added to the solution and stirred at 23°C overnight. The methanol was removed using a rotary evaporator. The residue was dissolved in 200 ml of CH_2Cl_2 acidified with 1 N HCl. The phases were separated and the aqueous layer was extracted again with CH_2Cl_2 . The organic phases were combined, washed with saturated NaCl, dried (MgSO_4), and concentrated to provide a white solid. The solid was recrystallized twice from ethyl acetate/hexane to give 34.7 g (0.136 mol, 96%) of compound **2** (*N*-benzenesulfonylproline). MS: m/z = 256.2 ($\text{M} + \text{H}^+$).

To a solution of 62 mg (0.27 mmol) of compound **1** and 77 mg (0.30 mmol) of compound **2** in 3 ml of dimethyl formamide (DMF) was



Scheme 1.

added 137 mg (0.36 mmol) of *O*-(7-azabenzotriazol-1-yl)-*N,N,N',N'*-tetramethyluronium hexafluorophosphate (HATU), followed by 175 μl (1.0 mmol) of diisopropylethylamine to give a yellow solution. After stirring at 23°C for 2 h, the solution was diluted with ethyl acetate, washed with 1 N HCl, then with 1 N NaOH, followed by a wash with saturated NaCl, and dried using Na_2SO_4 . The filtered solution was concentrated by vacuum to give 128 mg of compound **3** [2(*S*)-{[1-benzenesulfonyl-pyrrolidine-2(*S*)-carbonyl]-amino}-4-*tert*-utoxycarbonylamino-butyrac acid methyl ester] as a yellow oil, which was used without further purification. MS: m/z 470 ($M + H^+$), 370 ($M - \text{BOC} + H^+$); 75 mg (0.16 mmol) of compound **3** was dissolved in 3 ml of CH_2Cl_2 , and 1 ml of trifluoroacetic acid was added. After stirring for 2 h at 23°C, the solution was concentrated in CH_2Cl_2 3 times, and then dissolved in 2 ml of DMF; 56 mg (0.14 mmol) of amino acid **5** (Boc-*N*-Me-Lys(*Z*)-OH.DCHA (catalog no. A-3690; Bachem Bioscience, Inc., King of Prussia, PA), 64 mg (0.17 mmol) of HATU, and 175 μl (1.0 mmol) of diisopropylethylamine were added to give a yellow solution. This mixture was stirred for 4 h at 23°C, then diluted with ethyl acetate, washed with 1 N HCl, 1 N NaOH, then with saturated NaCl, and dried (Na_2SO_4). The filtered solution was concentrated by vacuum to give 100 mg (0.13 mmol, 96%) of compound **4** [2(*S*)-{[1-benzenesulfonyl-pyrrolidine-2(*S*)-carbonyl]-amino}-4-[6-benzyloxycarbonylamino-2(*S*)-(*tert*-utoxycarbonyl-methyl-amino)-hexanoylamino]-butyrac acid methyl ester] as a yellow

oil, which was used without further purification. MS: m/z 746 ($M + H^+$), 646 ($M - \text{BOC} + H^+$); 100 mg (0.13 mmol) of compound **4** was dissolved in 3 ml of CH_2Cl_2 ; a 1 ml aliquot of trifluoroacetic acid was added with stirring. After 2 h, the solution was redissolved in CH_2Cl_2 and concentrated three times, then dissolved in 3 ml of DMF; 43 mg (0.15 mmol) of *o*-methyl-tolyl-ureido-phenyl-acetic acid (PUPA)-OH, 64 mg (0.17 mmol) of HATU, and 175 μl (1.0 mmol) of diisopropylethylamine were added to give a yellow solution. After stirring at 23°C for 4 h, the solution was diluted with ethyl acetate and processed as described above for compound **4** to give a yellow foamy solid. Chromatography in (2:1 CH_2Cl_2 /acetonitrile, then 1:1 CH_2Cl_2 /acetonitrile, then 5% methanol in CH_2Cl_2 versus SiO_2) was performed to give 83 mg (0.09 mmol, 65%) of compound **6** [2(*S*)-{[1-benzenesulfonyl-pyrrolidine-2(*S*)-carbonyl]-amino}-4-[6-benzyloxycarbonylamino-2(*S*)-(methyl-{2-[4-(3-*o*-tolyl-ureido)-phenyl]-acetyl]-amino)-hexanoylamino]-butyrac acid methyl ester] ($R_f = 0.17$ in 1:1 CH_2Cl_2 /acetonitrile). MS: m/z 912 ($M + H^+$); 83 mg (0.09 mmol) of compound **6** was hydrogenated as above for compound **1**. The resulting solid was dissolved in 2 ml of DMF, and then 21 mg (0.09 mmol) of 6-(BOC-amino)caproic acid, 41 mg (0.11 mmol) of HATU, and 175 μl (1.0 mmol) of diisopropylethylamine were added. After stirring for 2 h at 23°C, the solution was diluted with ethyl acetate and processed as for compound **4**; 52 mg (0.05 mmol, 60%) of compound **6a** [2(*S*)-{[1-benzenesulfonyl-pyrrolidine-2(*S*)-carbonyl]-amino}-4-[6-(6-*tert*-utoxycarbonylamino-

hexanoylamino)-2(S)-(methyl-[2-[4-(3-*o*-tolyl-ureido)-phenyl]-acetyl]-amino)-hexanoylamino]-butyric acid methyl ester] was recovered as a yellow solid that was used without further purification. MS: m/z 991 ($M + H^+$), 891 ($M - BOC + H^+$).

To 52 mg (0.05 mmol) of compound **6a** in 3 ml of methanol, 265 μ l (0.53 mmol) of 2 N LiOH was added while stirring. After 2 h, the solution was redissolved in acetone and concentrated. The residue was dissolved in 2 ml CH_2Cl_2 , and 2 ml of trifluoroacetic acid was added. The sample was stirred for 90 min at 23°C and then concentrated. The residue was dissolved in minimal methanol and purified by reverse-phase high pressure liquid chromatography (5 to 95% acetonitrile in water with 0.1% trifluoroacetic acid) to give 26 mg (0.026 mmol, 50%) of compound **6b** [4-[6-(6-amino-hexanoylamino)-2(S)-(methyl-[2-[4-(3-*o*-tolyl-ureido)-phenyl]-acetyl]-amino)-hexanoylamino]-2(S)-[(1-benzenesulfonyl-pyrrolidine-2(S)-carbonyl)-amino]-butyric acid] (BIO8139) as a white solid. MS: m/z 878 ($M + H^+$).

Cell Adhesion Assays. The ability of BIO5192 to block $\alpha_2\beta_1$ /collagen I and $\alpha_9\beta_1$ /VCAM-1 interactions were evaluated in cell adhesion assays. Collagen I and VCAM-1 were immobilized onto a 96-well Corning Easy Wash plate (catalog no. 25801; Corning Inc., Corning, NY). Human integrin-expressing cell lines (2×10^5 /well) were labeled with a fluorescent compound, 2 μ M 2',7'-bis-(2-carboxyethyl)-5-(and-6)-carboxyfluorescein-acetoxymethyl ester (catalog no. B1150; Molecular Probes, Eugene, OR), and added plus or minus BIO5192. After 30 min, the plates were washed, and bound cells were quantified in a Cytofluor fluorescence plate reader. The assay buffer was TRIS-buffered saline (TBS: 24 mM TRIS, 137 mM NaCl, 2.7 mM KCl, 2 mM glucose, 0.1% BSA, pH 7.4), containing 1 mM $MnCl_2$. The specificity of binding was controlled for using integrin-specific neutralizing monoclonals. The antibodies were run at 10 μ g/ml on each day of assay and were as follows: anti- $\alpha_4\beta_1$, mAb HP1/2 (Biogen), anti- $\alpha_2\beta_1$, mAb 26G8 (Biogen) and $\alpha_9\beta_1$ -mAb Y9A2 (Chemicom).

Expression and Purification of VCAM-Ig and Direct Binding Assay Protocol. Details for the construction of the VCAM-Ig animal cell expression vector, the generation of a Chinese hamster ovary cell line expressing VCAM-Ig, conjugation of the VCAM-Ig to alkaline phosphatase, and the development of a direct binding assay for characterizing $\alpha_4\beta_1$ and $\alpha_4\beta_7$ binding to VCAM-Ig were as previously described (Lobb et al., 1995).

The $\alpha_{IIb}\beta_3$ -Fibrinogen Platelet Aggregation Assay. Whole blood (50 ml) was collected into 10-ml vacutainer tubes containing 1 ml of 3.8% sodium citrate. The citrate-treated blood was centrifuged for 5 min at 200g and the platelet-rich plasma was collected. Platelet-poor plasma was prepared by centrifuging the remaining blood specimen at 1500g for 15 min. The platelet count in the platelet-rich plasma was adjusted to 2×10^8 platelets/ml using the platelet-poor plasma. A Biodata 4-channel platelet aggregation profiler (PAP-4; Biodata Corp., Hatboro, PA) was blanked using a cuvette containing only platelet-poor plasma. Compounds in TBS containing 1 mM $MnCl_2$ (TBS-Mn) were tested at 100 μ M concentration. 350 μ l of platelet-rich plasma plus 100 μ l of compound were added to cuvettes containing stir bars and placed into the aggregometer. To start aggregation, 50 μ l of freshly made ADP at 2×10^{-4} M was added to each cuvette. A TBS-Mn control was run with each set of test samples. A 4-min aggregation tracing was generated for each sample and percent aggregation was calculated by the profiler. A positive control, 100 μ M of the RGD-containing peptide GRGDSP (Sigma-Aldrich, St. Louis, MO), was run on each day.

LIBS Assay. LIBS induction by BIO5192 was assessed in vitro by an adhesion assay. Corning Easy Wash 96-well plates were coated overnight at 4°C with the LIBS-recognizing mAb 9EG7 (catalog no. 09351D; BD Biosciences Pharmingen, San Diego, CA) (10 μ g/ml) in phosphate-buffered saline (PBS). The next day, plates were washed with PBS and blocked with 1% BSA in PBS for 1 h at 37°C. Jurkat cells (1×10^5 /well) were labeled with Calcein (Molecular Probes, Eugene, OR) at 37°C for 20 min in TBS, containing 2 mM $MgCl_2$ (Mg^{2+} -TBS) and washed twice. Calcein-labeled Jurkat cells were

added to wells either in Mg^{2+} -TBS or with serial dilutions of BIO5192 in Mg^{2+} -TBS. The plate was incubated for 30 min at 37°C; then the plates were washed three times with Mg^{2+} -TBS to remove unbound cells. The fluorescent cells that bound to mAb 9EG7 were analyzed by a Cytofluor fluorescence plate reader. Data reductions were done using Microsoft Excel 98.

Isolation of Peripheral Blood Lymphocytes (PBLs). Rat venous blood was collected in sodium citrate and centrifuged at 200g for 5 min. The platelet-rich plasma was discarded. The cell pellet was diluted 1:1 with Dulbecco's PBS without Ca^{2+} and Mg^{2+} (Sigma-Aldrich), layered onto Ficoll-Hypaque solution (Pharmacia, Peapack, NJ) and subjected to centrifugation at 900g for 20 min. The mononuclear cell layer at the plasma-Ficoll interface was collected. The cells were washed twice with RPMI 1640 medium containing 10% FBS (RPMI/10) with each step followed by centrifugation. The washed PBLs were resuspended in TBS-Mn.

Isolation of Splenocytes. Spleens were dissected from 240-g Lewis rats and gently forced through a 100- μ m mesh screen. Connective tissue was excluded from the cell suspension by the screen, and the resulting splenocytes were suspended in RPMI/10 medium. The cells were washed twice in RPMI/10 with each wash followed by a centrifugation step. Residual red blood cells in the splenocyte suspension were excluded from the cell count. Splenocytes (1.8×10^9) were obtained from a single spleen.

BIO8139-Biotin Occupancy FACS Assay. Splenocytes were isolated from control rats or from rats treated with BIO5192 (30 mg/kg, s.c.) or TA-2 (2.5 mg/kg, i.v.), as described above. Control rat splenocytes were incubated at 23°C for 15 min with a titration of either BIO5192 or TA-2 and washed twice with TBS-Mn with a centrifugation step between each wash. The samples were then incubated with 20 nM BIO8139-biotin at 23°C for 15 min, washed twice with TBS-Mn, treated with a 1:500 dilution of streptavidin-PE (catalog no. 016-110-084; Jackson ImmunoResearch Laboratories, Inc., West Grove, PA) for 15 min at 23°C, and again washed twice. The samples were resuspended in 200 μ l of assay buffer and analyzed by FACS. BIO8139-biotin was generated by reacting BIO8139 with biotin-PEG-CO₂-NHS, mol.wt. 3.4 kDa (Shearwater Polymers Inc., Huntsville, AL) and separating the modified BIO8139 from unmodified by size exclusion-HPLC on a Superdex peptide column (Amersham Biosciences, Inc., Piscataway, NJ). Where indicated in the text, this assay was replaced with a simpler version where BIO8139 was directly conjugated to the PE.

Monitoring $\alpha_4\beta_1$ Levels on PBLs and Splenocytes by FACS Analysis. Female Lewis rats were injected with a single dose of TA-2 (2.5 mg/kg, i.v. in PBS) or with PBS at 0 h, or two doses of BIO5192 (30 mg/kg, s.c. in TRIS/lactose) or vehicle at 0 and 24 h. The animals were sacrificed at 48 h. PBLs and splenocytes were isolated as described. BIO8139-PE (10 nM) or TA-2 (10 μ g/ml) followed by goat anti-mouse-PE, were added to the test samples and the cells were analyzed by FACS for the presence of cell surface $\alpha_4\beta_1$ integrin. In a separate experiment, samples were examined by FACS to determine the specific cell types present. The cells were analyzed using rat markers for T-cells, CD3 (catalog no. 22014D; BD Biosciences Pharmingen), and B-cells, CD45R (catalog no. 22164D; BD Biosciences Pharmingen), and their isotype-matched controls, IgG2b (catalog no. 03044C; BD Biosciences Pharmingen), and IgG3 (catalog no. 03064C; BD Biosciences Pharmingen).

PE-Labeled BIO8139 was prepared as follows: 200 μ l of 2.5 mM BIO8139, 5 mM succinimidyl-4-[*N*-maleimidomethyl]-cyclohexane-1-carboxylate sulfo-SMCC (Pierce Chemical, Rockford, IL), 100 mM HEPES, pH 7.5, in 90% dimethyl sulfoxide/10% water was incubated at 23°C for 4 h. Ethanolamine was added to 20 mM final to quench any further reaction and the BIO8139-SMCC conjugate was stored at -70°C for subsequent use. *R*-Phycoerythrin pyridylsulfide derivative (2 mg/ml, 1.8 pyridylsulfide residues/PE) was obtained from Molecular Probes. Three milliliters of the PE derivative was incubated with 10 mM DTT for 30 min at 23°C and desalted on a 35-ml G25M column in 5 mM MES, pH 5.5, and 100 mM NaCl. The PE

elution peak was collected visually and quantified by absorbance at 280 nm; 3.7 ml of 5 μ M PE was treated with 20 μ l of BIO8139-SMCC (10 μ M final) and 0.3 ml of 0.5 M MES, pH 6.5. The sample was incubated at 23°C for 2 h, then *N*-ethylmaleimide (Pierce Chemical) was added to 60 μ M, and the sample incubated further for 20 min. The sample was desalted on a 35-ml G25M column in 10 mM HEPES, pH 7.5, and 150 mM NaCl. The PE-BIO8139 conjugate was filtered through a 0.2- μ m filter and stored at 4°C. Batches were analyzed for relative potency by measuring dose-dependent staining on Jurkat cells by FACS analysis. Conjugates stored at 4°C were stable for about 2 months.

Assessing PK Properties of BIO5192 and TA-2 in Lewis Rats. Female Lewis rats, three per route of administration, received BIO5192 (30 mg/kg, s.c. or 1 mg/kg, i.v.) or TA-2 at 3 mg/kg, i.v. Blood samples (250 μ l/bleed) were obtained at specific time points after administration. For TA-2, blood samples were drawn at 0, 1, 2, 6, 8, 10, and 14 days. Serum samples were analyzed for TA-2 levels by ELISA. For BIO5192, blood samples were drawn at 0, 2, 6, 24, and 48 h. Serum samples were analyzed for BIO5192 levels using mass spectrometry. PK parameters were calculated from the mass spectrometry data by noncompartmental analysis. PK parameters include C_{MAX} (maximum serum concentration), t_{MAX} (time to achieve maximum serum concentration), CL (systemic clearance), V_{ss} (volume of distribution at steady state), $t_{1/2}$ (terminal phase half-life), and bioavailability. Area under the curve (AUC) was calculated using the trapezoidal rule. Percent bioavailability was calculated from the following equation: $(AUC_{extravasular}/AUC_{IV}) \times (Dose_{IV}/Dose_{extravasular}) \times 100$. For analysis of BIO5192 levels in serum by mass spectrometry, 100- μ l serum samples were extracted into methyl *tert*-butyl ether and spiked with an internal standard. Mass spectroscopy was performed on a Sciex API365 triple quadrupole mass spectrometer with a TurboIonSpray interface. The assay limit of quantification was 2 ng/ml.

TA-2 levels in serum were measured using a sandwich ELISA. Costar 96-well Easy Wash plates (Corning Inc.) were coated overnight at 4°C with 5 μ g/ml (50 μ l/well) of anti-AffiniPure goat-anti mouse IgG Fc fragment (Jackson ImmunoResearch Laboratories) in 50 mM sodium bicarbonate, pH 9.2. All subsequent manipulations were performed at room temperature. The plates were blocked for 30 min with 200 μ l/well 1% BSA (cat. no. A-7030; Sigma-Aldrich) in 10 mM Tris-HCl, pH 7.5, 150 mM NaCl, 0.05% Tween 20, 0.01% thimerosal, and washed three times with TBS (50 mM Tris-HCl, pH 7.5, 150 mM NaCl). The wells were then treated for 1 h with serial dilutions of PK samples or of the appropriate dosing solution standards (50 μ l/well) diluted in blocking buffer plus 1% rat plasma. The plates were washed three times and incubated for 1 h with 50 μ l/well of goat anti-mouse IgG1-alkaline phosphatase (catalog no. 1070-04; Southern Biotechnology Associates, Inc., Birmingham, AL) at a 1:2000 dilution in blocking buffer plus 1% rat plasma (100 μ l/well). The plates were again washed three times, incubated for 1 h with 5 mg/ml 4-nitrophenyl phosphate in 100 mM glycine, pH 10.5, 1 mM $ZnCl_2$, 1 mM $MgCl_2$, and read at 405 nm on a Molecular Devices Thermo Max microplate reader. Each sample was analyzed in duplicate, and three animals were analyzed per time point. TA-2 concentrations were calculated by interpolation from a standard curve.

Assessing Lymphocyte Counts and Subtypes following Inhibitor Treatments. Female Lewis rats were injected with a single dose of either TA-2 (2.5 mg/kg, i.v. in PBS), or BIO5192 (30 mg/kg, s.c., in TRIS/lactose) or with their respective vehicles at time 0. At each time point, 0.3 ml of blood from triplicate animals was drawn from the jugular vein without anesthesia using indwelling catheters and collected into Capiject purple-top microtainer tubes containing EDTA (catalog no. T-MQK; Terumo Medical Corp., Somerset, NJ). Plasma samples were analyzed for lymphocyte count using an Abbott CellDyn 3500 cell analyzer (Abbott Diagnostics, Abbott Park, IL). Blood samples from the TA-2-treated animals were drawn on days 1, 2, 4, 6, 8, 10, and 14 and for the BIO5192-treated animals after 2, 6, 24, and 48 h.

Rat EAE Model. Healthy female Lewis rats weighing 150 g were obtained from Harlan (Indianapolis, IN) and housed in ventilated cage racks and allowed food and water ad libitum. At approximately 9 weeks of age, animals were immunized with an emulsion of guinea pig myelin basic protein (MBP) peptide in complete Freund's adjuvant. MBP peptide sequence of GPMBPYGSLPQKSQRSDENPV (amino acid residues 68–86), 100 μ g/ml in PBS, was diluted with an equal volume of incomplete Freund's adjuvant. Before emulsification, ground *Mycobacterium tuberculosis* was added to 4 mg/ml. Animals were anesthetized with isoflurane and immunized with a single footpad injection of 100 μ l of the emulsion. Animal body weights, and observations for signs of paralysis starting on day 8 post immunization, were collected daily. Each treatment group contained 13 animals. BIO5192 was administered at 30 mg/kg in TRIS/lactose, s.c., b.i.d., during days 5 through 14. Untreated rats and TRIS/lactose vehicle-treated controls were also monitored. For TA-2 treatment, rats were injected i.v. on day 9 and day 13 with TA-2 (2.5 mg/kg). The following grading system was used to quantify disease severity: 0.5 = half of tail limp; 1.0 = whole tail limp; 1.5 = whole tail limp with a small amount of gait disruption; 2.0 = hind limb weakness (waddling gait or one dragging leg); 2.5 = hind limb weakness (one dragging leg with a small amount of loss of motile function in opposite leg); 3.0 = hind limb paralysis (both legs dragging; some slight hind limb movement); 3.5 = hind limb paralysis (both legs dragging with a small amount of forelimb weakness); 4.0 = hind limb and front limb paralysis (sufficient to prevent movement); 5.0 = moribund or death. Statistical significance of differences in severity of disease (peak height) and day of peak disease score (peak day) were assessed using a one-way analysis of variance followed by Fisher's protected least significant difference test for multiple comparisons among means. *P* values of less than 0.05 were taken to be statistically significant. All procedures using animals were conducted in accordance with the *National Institutes of Health Guide for the Care and Use of Laboratory Animals* and approved by the Institutional Animal Care and Use Committee.

Assessing $\alpha_4\beta_1$ Expression by Confocal Microscopy. TA-2 and BIO8139 were conjugated with AlexaFluor594 (Molecular Probes, Inc.) following the manufacturer's instructions. The BIO8139-Alexa594 conjugate was generated by first reacting BIO8139 with NHS-PEG-maleimide 2.4 K (Shearwater Polymers Inc.), then treating the BIO8139-PEG with sonic hedgehog (Shh) protein that contains a single thiol for modification, and finally reacting the BIO8139-PEG-Shh with Alexa594. RBL.1 cells were incubated with TA-2-Alexa594 (10 μ g/ml) or BIO8139-Alexa594 (50 nM) for 30 min at 4°C. The cells (100,000 cells/well) were plated onto a 96-well flat-bottomed plate in Earle's minimal essential medium, 10% FBS, 1 mM sodium pyruvate, and further incubated with the inhibitors at 37°C for either 0 or 48 h. The cells were washed and fixed in 2% paraformaldehyde at designated time points. Freshly isolated rat splenocytes were incubated with unlabeled TA-2. Splenocytes were washed and fixed in 2% paraformaldehyde following 0, 4, 24, and 48 h of continual TA-2 treatment at 37°C. Cell suspensions were permeabilized using the Cytoperm/cytofix kit (BD Bioscience Pharmingen) and incubated with goat anti-mouse-Alexa594. The cells were placed onto slides with coverslips and fluorescence detection of the Alexa594-labeled complex $\alpha_4\beta_1$ /inhibitor was analyzed by confocal laser-scanning microscopy using a Leica TCS SP confocal microscope equipped with a krypton/argon/helium/neon laser (Leica Lasertechnik GmbH, Heidelberg, Germany). For Alexa594 staining, red channel (600–700 nm range) images were collected from the center of representative cells showing intact cell membranes.

Results

Characterization of the Biochemical Properties of BIO5192. The small molecule inhibitor BIO5192 was identified as a potent inhibitor of $\alpha_4\beta_1$ ($K_D < 10$ pM) from a

structure-activity relationship analysis of $\alpha_4\beta_1$ inhibitors (D. M. Scott, manuscript in preparation). The high affinity for $\alpha_4\beta_1$ results from an extremely slow dissociation rate of the inhibitor from the integrin/inhibitor complex, with a dissociation half-life of >12 h for both the unactivated and activated integrin. The following studies were performed to further characterize the properties of BIO5192. First, the selectivity of BIO5192 for $\alpha_4\beta_1$ was evaluated by assessing the binding of BIO5192 to cells expressing $\alpha_4\beta_7$, $\alpha_9\beta_1$, $\alpha_2\beta_1$, and $\alpha_{IIb}\beta_3$ (Table 1). BIO5192 was highly selective for $\alpha_4\beta_1$. The affinity of BIO5192 for $\alpha_4\beta_1$ was 250- to 1000-fold higher than for the related integrin, $\alpha_4\beta_7$, which shares many of the same ligands as $\alpha_4\beta_1$. The inhibitor bound even less tightly to the same ligands as $\alpha_4\beta_1$. The inhibitor bound even less tightly to $\alpha_2\beta_1$ and $\alpha_{IIb}\beta_3$ (Table 1). A low but significant level ($K_D = 140$ nM) of binding was seen on $\alpha_9\beta_1$ integrin in buffer containing 1 mM Mn^{2+} . The large discrepancy in the binding constants calculated from the adhesion assay shown in Table 1 ($IC_{50} = 1.8$ nM) and from the kinetic data ($K_D < 10$ pM) (Scott, 2002; manuscript in preparation) arise because the affinity constant of BIO5192 for $\alpha_4\beta_1$ is lower than the concentration of $\alpha_4\beta_1$ in the binding assay. Consequently, the IC_{50} data reflect the concentration of $\alpha_4\beta_1$ in the adhesion assay and not the affinity of BIO5192 for $\alpha_4\beta_1$, as discussed elsewhere (Pepinsky et al., 2002).

Second, the effects of protein binding on the affinity of BIO5192 for $\alpha_4\beta_1$ were evaluated in vitro by kinetic measurements using a radiolabeled analog of BIO5192, [^{35}S]BIO7662 (Chen et al., 2001). Figure 1A shows association curves for the binding of [^{35}S]BIO7662 to Jurkat cells ($\alpha_4\beta_1$ positive) in TBS buffer containing 1 mM Ca^{2+} and 1 mM Mg^{2+} alone, and in the same buffer with increasing amounts of plasma. The association rate for BIO7662 binding to $\alpha_4\beta_1$ decreased with increasing plasma concentrations. This effect was caused by nonspecific binding of [^{35}S]BIO7662 to serum albumin and can be mimicked by incubating samples with the corresponding concentration of albumin (data not shown). As the amount of plasma was increased from 20 to 100%, the effective concentration of [^{35}S]BIO7662 diminished, causing a decline in the association rate for the binding of BIO7662 to $\alpha_4\beta_1$. Plasma binding had no effect on the dissociation rate constant for the release of [^{35}S]BIO7662 from $\alpha_4\beta_1$ /[^{35}S]BIO7662 complexes (data not shown). Although protein binding in general reduces the effective concentration of a compound, for tight binding inhibitors such as BIO5192 a slow off-rate drives the binding equilibrium toward the occupied state and therefore in part compensates for the apparent loss in concentration due to protein binding.

TABLE 1

Integrin selectivity data for BIO5192

The selectivity of BIO5192 toward the five integrins indicated were tested in adhesion formats for $\alpha_9\beta_1$ and $\alpha_9\beta_1$ by direct binding for $\alpha_4\beta_1$ and $\alpha_4\beta_7$, and by platelet aggregation for $\alpha_{IIb}\beta_3$, as described under *Materials and Methods*. For all assay formats, serial dilutions of each compound (from 1 nM to 100 μ M) were evaluated and IC_{50} values were calculated from the concentration dependence of the inhibition curves.

Integrin	IC_{50} (n)
	nM
$\alpha_4\beta_1^a$	1.8 ± 0.7 (10)
$\alpha_4\beta_7$	>500 (1)
$\alpha_9\beta_1$	138 (2)
$\alpha_2\beta_1$	$1,053 \pm 143$ (3)
$\alpha_{IIb}\beta_3$	>10,000 (1)

^a Due to the high affinity of BIO5192 for $\alpha_4\beta_1$, its binding constants were also calculated from kinetic measurements ($K_D = <10$ pM).

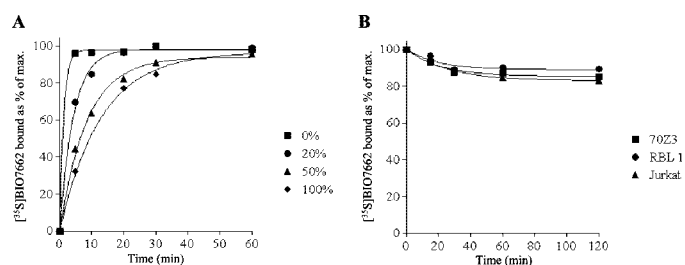


Fig. 1. Assessing binding of [^{35}S]BIO7662 to cells expressing $\alpha_4\beta_1$ using kinetic measurements. For assessing binding of BIO5192 to $\alpha_4\beta_1$ -expressing cells the radiolabeled derivative of BIO5192, [^{35}S]BIO7662, was used as described previously (Chen et al., 2001). A, for on-rate measurements, Jurkat cells (1×10^6 cells/ml) in TBS containing 1 mM Ca^{2+} and 1 mM Mg^{2+} plus varying amounts of rat plasma: 0% (■), 20% (●), 50% (▲), or 100% (◆) were treated with 2 nM [^{35}S]BIO7662 for 5, 10, 20, 30, or 60 min. Cells were collected by centrifugation and subjected to scintillation counting. The data were fitted to an exponential equation by nonlinear regression. B, for off-rates, cells expressing $\alpha_4\beta_1$: 70Z3 cells (■), RBL.1 cells (●), or Jurkat cells (▲) at 1×10^6 cells/ml were treated with 5 nM [^{35}S]BIO7662 for 40 min in TBS containing 1 mM Ca^{2+} and 1 mM Mg^{2+} . Unlabeled BIO7662 (500 nM) was added, and the cells were further incubated for the times indicated in the presence of 1 mM Ca^{2+} and 1 mM Mg^{2+} buffer. Cells were pelleted at each time point, and cell-associated [^{35}S]BIO7662 was measured by scintillation counting. Dissociation data are represented as a percentage of the maximum total counts bound as a function of time. The data were fitted to a single exponential for all curves. k_{on} and k_{off} values were calculated from the curve fits. k_{off} is the observed rate constant; k_{on} is the observed binding constant divided by the concentration of BIO7662. Data shown are from a single determination of the on and off rates.

Third, the ability of BIO5192 to recognize $\alpha_4\beta_1$ from different species was tested by using kinetic measurements to calculate affinity constants. On and off-rate measurements for binding and dissociation of [^{35}S]BIO7662 for human, rat, and mouse cells were similar. Figure 1B shows the dissociation curves for the binding of [^{35}S]BIO7662 from $\alpha_4\beta_1$ on human Jurkat, rat RBL.1 and mouse 70Z3 cells in buffer containing 1 mM Ca^{2+} and 1 mM Mg^{2+} . The $\alpha_4\beta_1$ receptors from the three species all remained 90% saturated with [^{35}S]BIO7662 at 120 min, demonstrating a slow dissociation rate. Off rates of $\leq 0.19 \times 10^{-4} s^{-1}$ were calculated from the dissociation data. Binding in the presence of 1 mM Mn^{2+} changed the $\alpha_4\beta_1$ integrin to a higher activation state (Chen et al., 2001). The dissociation of [^{35}S]BIO7662 from $\alpha_4\beta_1$ in the presence of 1 mM Mn^{2+} was too slow to allow determination of an accurate k_{off} , but extrapolation from the available data suggests a half-life for dissociation of at least 16 h, corresponding to a $k_{off} \leq 0.11 \times 10^{-4} s^{-1}$ (data not shown). Since $k_{on} = 1.9 \times 10^6 M^{-1} s^{-1}$ for the binding of BIO7662 to the unactivated integrin, the resulting K_D that was calculated from k_{on} and k_{off} is 10 pM or less for rat, mouse, and human $\alpha_4\beta_1$.

Fourth, the ability of BIO5192 binding to induce expression of LIBS epitopes was evaluated. Ligand binding induces a cascade of conformational changes within the integrin that has been studied in detail using mAbs whose epitopes are either exposed (termed LIBS; also referred to as CLIBS due to modulation of the epitope by cations) or lost following ligand binding (Humphries, 1996; Newham et al., 1998). Monoclonal antibody 9EG7 recognizes and binds to exposed epitopes on the β_1 chain of $\alpha_4\beta_1$ that are presented when the ligand binding site is occupied. BIO5192 induced binding of 9EG7 with an EC_{50} of approximately 0.3 nM indicating that BIO5192 is a LIBS inducer. The EC_{50} for BIO5192 LIBS

induction (Fig. 2) and the nanomolar potency in the binding assay were similar.

In Vivo Measurements of the Binding of BIO5192 to Rat Lymphocytes. To compare the treatment effects of BIO5192 and TA-2 in a rat EAE model, the PK and PD properties of the two inhibitors were evaluated to select appropriate dosing regimens. First, the binding of BIO5192 and TA-2 to $\alpha_4\beta_1$ was measured on freshly isolated rat PBLs. These titration curves are shown in Fig. 3A. The binding of BIO5192 and TA-2 on PBLs was dose-dependent and saturable; TA-2 had a 2- to 3-fold higher apparent binding affinity. The binding of BIO5192 to isolated rat splenocytes is shown in Fig. 3B. The binding is dose-dependent and saturable with an IC_{50} of 1 nM.

The in vivo time course of receptor occupancy was studied using rat splenocytes ex vivo to characterize binding. Figure 3C shows the results from a study in which female Lewis rats were treated with a single dose of BIO5192 at 30 mg/kg, s.c., at $t = 0$ min, and splenocytes were harvested at 24, 48, and 72 h and assayed for receptor occupancy. At 24 h, all $\alpha_4\beta_1$ receptors were occupied by BIO5192. After 48 h, 50% remain occupied, and at 72 h, less than 40% were occupied. Blood levels of BIO5192 in these animals as measured by mass spectroscopy were 180 ng/ml at 24 h but were below limits of detection (≤ 2 ng/ml) at 48 and 72 h. These data demonstrate that BIO5192 remains bound to the $\alpha_4\beta_1$ receptor even in the absence of circulating plasma levels of compound and suggest that the slow off-rate for BIO5192 that was observed in vitro also occurs in vivo. This hypothesis was supported by leukocytosis data that was routinely used as an in vivo PD marker for receptor occupancy (see below).

Pharmacokinetics of BIO5192 and TA-2 in Female Lewis Rats. The pharmacokinetic properties of BIO5192 were evaluated by noncompartmental analysis following i.v.

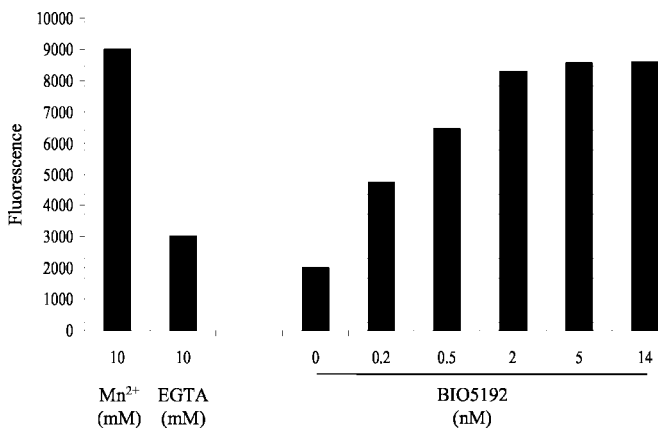


Fig. 2. Induction of the expression of the 9EG7 LIBS epitope by BIO5192. The effects of BIO5192 on the expression of the LIBS epitope that can be detected with the 9EG7 mAb were evaluated on Jurkat cells expressing $\alpha_4\beta_1$ in an adhesion assay. Calcein-labeled Jurkat cells (1×10^5 cells) in TBS plus 2 mM Mg^{2+} were incubated for 30 min at 37°C with serial dilutions of BIO5192 or EGTA at the various concentrations indicated. Costar 96-well Easy Wash plates were coated with 10 μ g/ml 9EG7 and blocked with bovine serum albumin. Plates were washed three times and read on a CytoFluor 4000 multiwell plate reader from Applied Biosystems (Foster City, CA) (excitation at 485 nm, emission at 530 nm). For $\alpha_4\beta_1$ cells, background binding was 400 mean fluorescence units and maximum binding was 9000 units. 0% = nonspecific binding to non-9EG7 coated wells. 100% = binding seen in the presence of 14 nM BIO5192. As a further control for LIBS induction, certain wells were treated with Mn^{2+} , which itself is a potent inducer of the LIBS epitope. As expected Mn^{2+} induced expression of the LIBS epitope on Jurkat cells.

or s.c. administration in female Lewis rats (Fig. 4). BIO5192, dosed at 1 mg/kg, i.v. showed a multiexponential disposition with a rapid initial decline followed by a less steep terminal phase. The terminal half-life was 1.1 h. Prolonged exposure was observed following s.c. administration. Dose-dependent increases in available drug were observed with C_{MAX} occurring from 30 to 60 min in all treatment groups. Half-lives of 1.7, 2.7, and 4.7 h were observed for the 3, 10, and 30 mg/kg, s.c. doses, respectively. The blood plasma curves show that the AUC for the s.c. route of administration increased about 2.5-fold from 5,460 h \times ng/ml for the 3 mg/kg dose to 14,175 h \times ng/ml for the 30 mg/kg dose. Following the 30 mg/kg, s.c. dosing, blood levels of >100 ng/ml were maintained for over 24 h, and consequently, once a day dosing at 30 mg/kg was chosen for all subsequent studies. The increase in the half-life of BIO5192 at the 30 mg/kg dose relative to the half-life at lower doses is the result of a depot effect. At this high dose, dissolution of the BIO5192 results in a slow release of the compound into the bloodstream.

TA-2 was administered i.v. to rats at 2.5 mg/kg for determination of half-life (Fig. 5). Levels of antibody of >2 μ g/ml were observed for 7 days. Based on the data, a $t_{1/2}$ of 2 days was calculated.

Comparative Pharmacodynamics of BIO5192 and TA-2 in Rats. Administration of BIO5192 and TA-2 to rats produced a lymphocytosis that was sustained as long as sufficient concentrations of the inhibitors were maintained in circulation to provide $>90\%$ of $\alpha_4\beta_1$ receptors occupied. Figure 5A shows lymphocytosis induced in vivo by TA-2 treatment. A 3- to 4-fold increase in lymphocyte levels was observed. The maximal level of induction was reached at the earliest time point tested, after 24 h. Elevated lymphocyte levels were maintained for 6 days with the half maximum occurring on day 7. The elimination half-life of TA-2 is 2 days. The biological effect of the TA-2 antibody was clearly associated with its PK. At 7 days, the TA-2 blood level had dropped to 2 μ g/ml, and by 8 days there was no detectable TA-2 in the blood. During the analysis of the lymphocyte levels, circulating differential white blood cell counts were examined from three animals on day 1 and day 10 following TA-2 treatment. Lymphocyte levels increased from a baseline of $6,800 \pm 300$ to $18,400 \pm 400/\mu$ l (mean \pm S.E.M.) on day 1 and returned to baseline on day 10. Basophil levels increased to $50 \pm 20/\mu$ l on day 1 and returned to normal levels of $8 \pm 1/\mu$ l by day 10. Levels of neutrophils ($600 \pm 40/\mu$ l, day 1; $900 \pm 70/\mu$ l, day 10), monocytes ($300 \pm 50/\mu$ l, day 1; $300 \pm 20/\mu$ l, day 10), and eosinophils ($20 \pm 2/\mu$ l, day 1; $40 \pm 10/\mu$ l, day 10) did not change in response to TA-2 treatment.

Figure 5B shows the pharmacodynamic effect of BIO5192. The lymphocyte count rose about 1.5-fold after 24 h of drug treatment. Half as many cells were released into the circulation following BIO5192 treatment as when TA-2 was given. The transient leukocytosis was sustained for 30 h. The observed $t_{1/2}$ of BIO5192 is approximately 12 h. Although the PK data would suggest that lymphocytosis should have been reversed at an earlier time, the receptor occupancy study described above showed that BIO5192 remains bound to 100% of the $\alpha_4\beta_1$ receptors for 24 h and 50% bound for 48 h, even in the absence of compound plasma levels. These data demonstrate that the slow dissociation rate and prolonged receptor occupancy of BIO5192 is associated with a biological

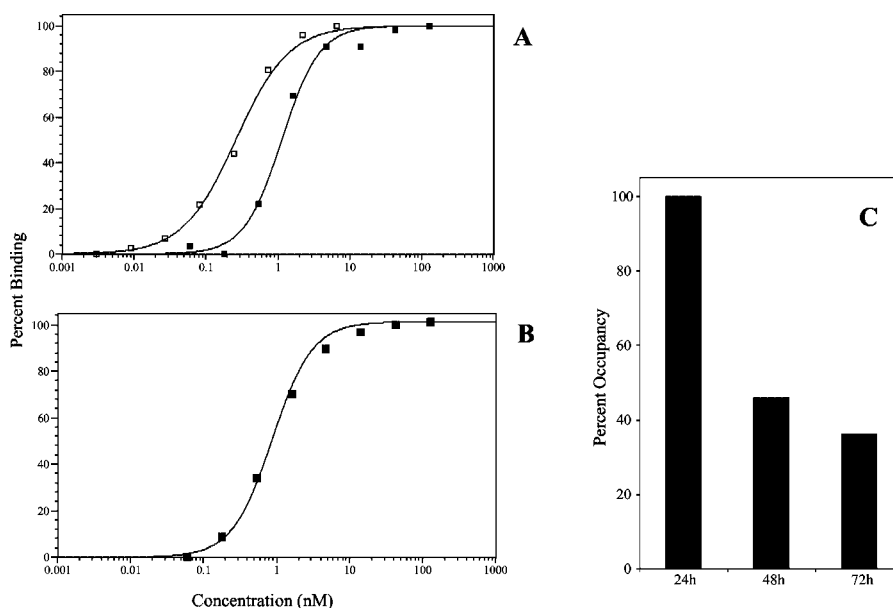


Fig. 3. Assessing the occupancy of $\alpha_4\beta_1$ integrin receptors. Binding of BIO5192 and TA-2 to rat PBLs (A) and BIO5192 binding to rat splenocytes (B) in vitro and BIO5192 splenocyte receptor occupancy following an in vivo administration (C) were investigated. 4.0×10^6 cells/ml of PBLs (A) or splenocytes (B) were incubated at 23°C for 30 min with the indicated concentrations of BIO5192 (■) in the presence of TBS containing 1 mM Mn^{2+} or TA-2 (□) in the presence of TBS containing 1 mM Ca^{2+} and 1 mM Mg^{2+} . The cells were washed and pelleted by centrifugation. BIO8139-PE (10 nM) was added to the cells treated with the BIO5192 titration, and goat anti-mouse-PE (1:500) was added to the cells treated with the TA-2 titration, then incubated at 23°C for 30 min. Cells were collected by centrifugation and subjected to FACS analysis. Solid lines represent best fit of the data to a hyperbolic equation. C, rats were injected once with BIO5192 (30 mg/kg, s.c.) at time 0. At 24, 48, and 72 h post injection of BIO5192, splenocytes were isolated and 4.0×10^6 /ml of splenocytes were incubated with BIO8139-PE (10 nM) for 15 min. Cells were washed and collected by centrifugation and subjected to FACS analysis. Data are the mean of two animals.

activity that occurs in the absence of compound plasma levels.

TA-2 and BIO5192 Treatments Delay Paralysis Associated with EAE. EAE was induced in female Lewis rats with MBP peptide. The time course for EAE is shown in Fig. 6. The effects of the MBP treatment on the paralytic score were monitored from day 8 to day 26. The earliest onset of paralysis in the no treatment and TRIS/lactose vehicle control groups occurred on day 9 followed by a peak of disease between days 12 and 13 with a paralytic score of 3. The disease resolved to a baseline paralysis score of 0 by day 18. There was a decrease in body weight during the course of the disease and a return to normal following the resolution of EAE. TA-2 treatment following injections on days 9 and 13 (2.5 mg/kg, i.v.) resulted in a 3- to 4-day delay in onset of the disease and a decrease in total disease severity. With a half-life of 2 days, we expected that sufficient blood levels of TA-2 would last 7 days and therefore that dosing on days 9 and 13 would be an effective treatment regimen. This result is evident from the plotted data. Rats treated with BIO5192 (30 mg/kg, s.c.) also show a 3-day delay in onset of disease when dosed b.i.d. (Fig. 6), and a 1- to 2-day shift when dosed q.d. (data not shown) compared with the control groups. The delay in onset of the disease in the BIO5192 treatment group is consistent with the finding that bound BIO5192 will occupy $\alpha_4\beta_1$ long beyond the point at which the BIO5192 is no longer detected in blood. Once BIO5192 is released, EAE underwent its normal disease progression. The disease in rats from both the TA-2 and BIO5192 treatment groups reached a paralytic score of 2.0, indicating that both inhibitors delayed the onset and decreased the severity of the disease.

The statistical significance of differences in severity of

disease (peak height) and day of peak disease score (peak day) were assessed using a one-way analysis of variance followed by Fisher's protected least significant difference test. In a comparison of the day of peak disease for treated versus controls, P values of <0.0001 were obtained for BIO5192 treatment versus both vehicle and untreated controls, and similarly, P values of <0.0001 were obtained for TA-2 treatment versus vehicle and untreated controls. Statistical differences in disease severity (peak height) were also compared. P values of <0.0032 were observed for peak height for BIO5192 versus both the vehicle and the untreated controls, and P values <0.0011 were obtained for the TA-2-treated group versus the two control groups.

TA-2 Treatment Down-Modulates $\alpha_4\beta_1$ Surface Expression. As part of the analysis of function, we tested whether TA-2 or BIO5192 modulated $\alpha_4\beta_1$ levels in vivo. For these studies, female Lewis rats were treated with either a single 2.5 mg/kg dose of TA-2 at $t = 0$ h or with 2 doses of BIO5192 at 30 mg/kg at $t = 0$ and $t = 24$ h. Freshly isolated rat PBLs and splenocytes were analyzed at $t = 48$ h for receptor levels and occupancy. Figure 7 shows the results from this analysis. PBLs and splenocytes from the vehicle-treated control animals showed strong FACS signals when analyzed by ex vivo treatment with TA-2 and detected with anti-mouse PE or by direct analysis using a PE-tagged analog of BIO5192, PE-BIO8139. When animals were treated with BIO5192 and analyzed for receptor occupancy using PE-BIO8139, no binding of the analog was observed. To rule out modulation of the receptor, we analyzed the cells from the BIO5192-treated rats with TA-2 and measured $\alpha_4\beta_1$ levels using a PE-labeled anti-mouse antibody. No change in receptor number was observed for the BIO5192-treated animals versus the untreated control animals, indicating that the loss

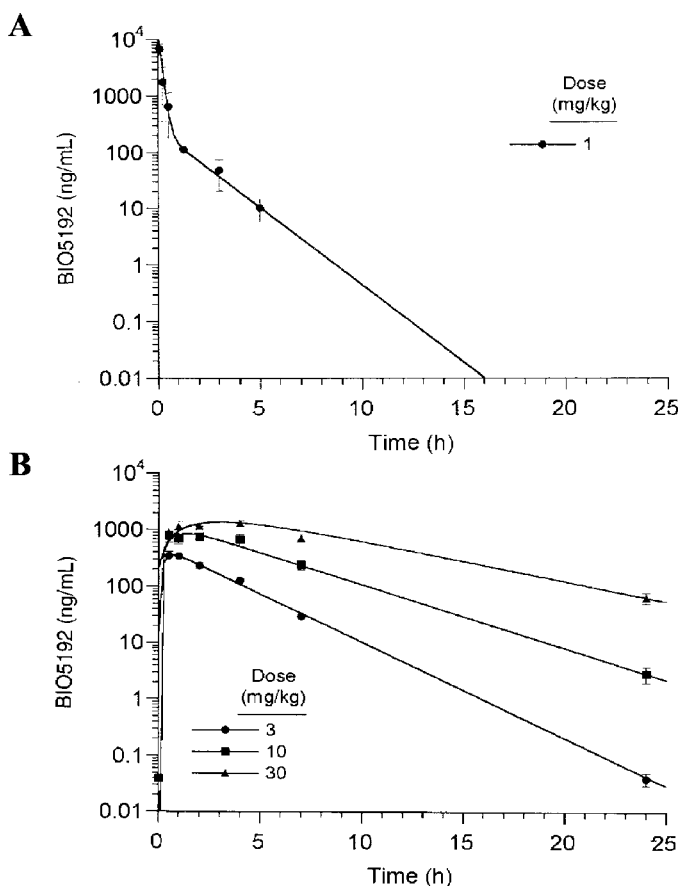


Fig. 4. Pharmacokinetic analysis of BIO5192 in Lewis rats following i.v. and s.c. administration. Rats were injected with BIO5192 at 1 mg/kg, i.v. (●) (top panel), or with 3 (●), 10 (■), or 30 (▲) mg/kg, s.c. (bottom panel). Whole blood from these animals was collected and treated with heparin at the time points indicated. BIO5192 was isolated from the resulting plasma by extraction and BIO5192 levels were assessed by mass spectroscopy (see *Materials and Methods*). Each curve is the mean of data from three animals. Data are expressed as mean \pm S.D.

of signal with PE-BIO8139 was due to the presence of bound BIO5192. This observation is consistent with the finding that BIO5192 dissociates slowly from $\alpha_4\beta_1$ and remains bound after 24 h. The cells isolated from the TA-2-treated group were analyzed for TA-2 binding using anti-mouse PE. With a half-life of 48 h, we had expected to observe full saturation of $\alpha_4\beta_1$ receptors by TA-2 but instead no bound TA-2 was observed (data not shown). To explain this observation, the cells from this group were treated ex vivo with TA-2 detected with anti-mouse PE or with PE-BIO8139 and directly analyzed for binding by FACS. In both instances, there was little or no signal observed indicating that no appreciable $\alpha_4\beta_1$ receptor level was present (Fig. 7). A PK study was conducted separately to examine the $\alpha_4\beta_1$ levels on PBLs and splenocytes following a single injection of TA-2 administered to Lewis rats. Cells were isolated on days 1, 2, 4, 6, 8, 10, and 14 and the presence of $\alpha_4\beta_1$ on the cells was analyzed using TA-2 detected with goat anti-mouse PE and compared with TA-2 serum levels. On days 1, 2, and 4 there was no $\alpha_4\beta_1$ present on the lymphocytes. The serum TA-2 concentrations were between 8 and 25 $\mu\text{g/ml}$ on days 4 and 1, respectively. At day 6, when the serum TA-2 level was at 2 $\mu\text{g/ml}$, the $\alpha_4\beta_1$ levels began to rise and reached a half-maximal signal by day 8, when the serum TA-2 had dropped to <1 $\mu\text{g/ml}$. Cell surface

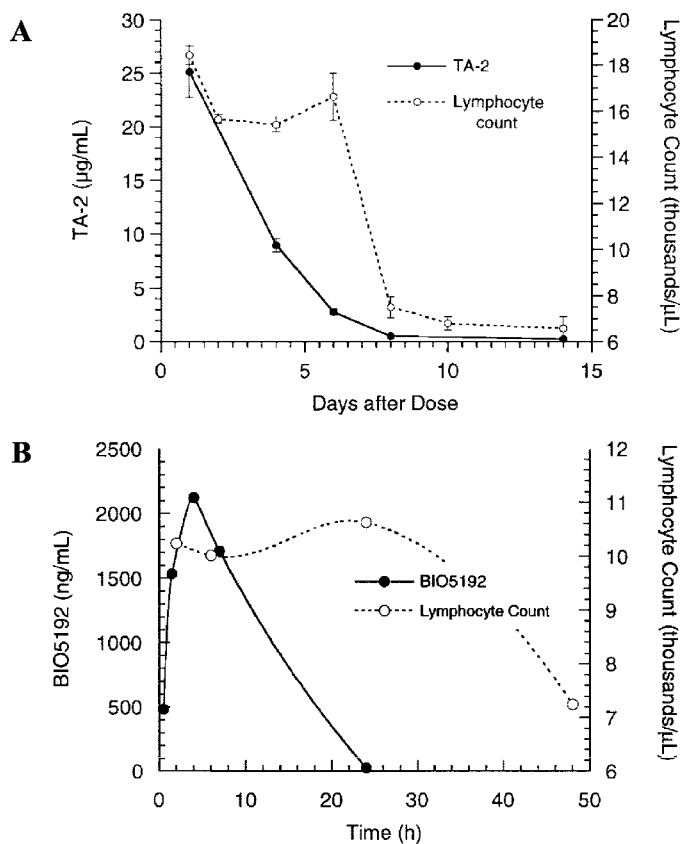


Fig. 5. Pharmacodynamic effects of $\alpha_4\beta_1$ inhibitors. A single dose of TA-2 (2.5 mg/kg, i.v. in PBS), BIO5192 (30 mg/kg, s.c. in TRIS/lactose), or the corresponding vehicle control was administered to Lewis rats at time 0. Blood was collected into EDTA to form plasma at the time points indicated and analyzed for circulating blood count (CBC) by a CellDyne cell analyzer. Lymphocyte counts were assessed for each animal from the CBC. The top panel shows the lymphocyte counts (○) following TA-2 injection relative to PK data for TA-2 (●), which was measured in the same study. The bottom panel shows the lymphocyte counts (○) following BIO5192 injection in relation to its PK data (●). Data points are the mean of three animals \pm S.D.

$\alpha_4\beta_1$ levels returned to normal by day 14 when the serum TA-2 level had fallen below the limits of detection of the assay (data not shown). Additionally, we and others (P. Kubes, unpublished observations) have observed that a mouse-specific $\alpha_4\beta_1$ mAb, PS/2, down-modulated $\alpha_4\beta_1$ on PBLs and splenocytes isolated from treated mice (data not shown). Whereas treatment with the PE-BIO8139 probe verified that there was no free $\alpha_4\beta_1$ on the cells isolated from TA-2-treated animals, the PE label sterically interferes with the binding of BIO8139 to $\alpha_4\beta_1$ that is bound to TA-2. This interference does not occur if the [^{35}S]BIO7662 probe is used. Consequently, we also tested binding to $\alpha_4\beta_1$ on cells isolated from rats treated with either TA-2 or BIO5192 using the [^{35}S]BIO7662 probe. Specific binding was observed on cells isolated from untreated rats and from the same cells treated with TA-2, ex vivo. In contrast, only background binding of the probe was observed on cells from animals treated with TA-2 or BIO5192 (data not shown). The loss of [^{35}S]BIO7662 binding on cells isolated from TA-2-treated animals, but not on cells from untreated animals that were incubated with TA-2 in vitro, further verifies that TA-2 treatment down-modulates $\alpha_4\beta_1$ expression. To rule out the selective loss of a lymphocyte subtype, PBLs isolated from the TA-2-treated

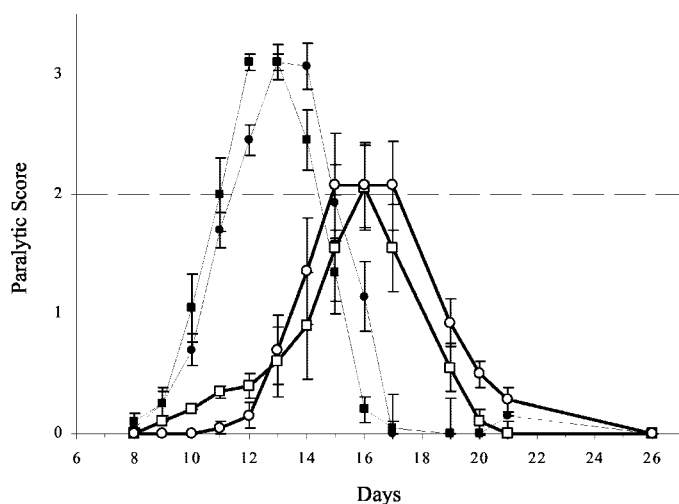


Fig. 6. Evaluation of BIO5192 and TA-2 in rat EAE. Lewis rats were injected with MBP on day 0 and then monitored daily for progression of the disease. The treatment groups receiving either no treatment (■), the TRIS/lactose vehicle (●), TA-2 (2.5 mg/kg, i.v., day 9 and 13) (□), or BIO5192 (30 mg/kg, s.c.) administered b.i.d. during days 5 through 14 (○). Values are given as the mean \pm S.D. for 13 animals.

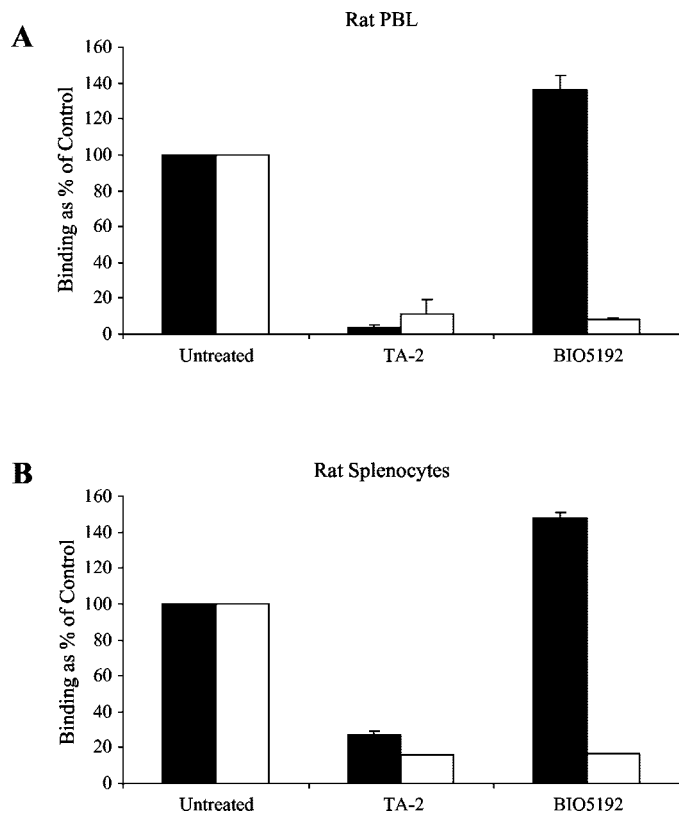


Fig. 7. Modulation of $\alpha_4\beta_1$ integrin by TA-2 but not BIO5192. A single dose of TA-2 (2.5 mg/kg, i.v. in PBS), BIO5192 (30 mg/kg, s.c. in TRIS/lactose, QD) or the corresponding vehicle control was administered to Lewis rats at time 0. After 48 h, PBLs and splenocytes were isolated and analyzed for $\alpha_4\beta_1$ levels by FACS analysis. 100% represents the binding seen in vehicle-treated animals. The solid bars represent cells treated with additional TA-2 (10 μ g/ml) followed by goat anti-mouse-PE, and the open bars represent cells treated with BIO8139-PE, for detection of cell surface $\alpha_4\beta_1$.

and untreated animals were analyzed by FACS using specific surface markers for T- and B-cells. At 24 h post TA-2 treatment, the percentage of total cells versus the untreated con-

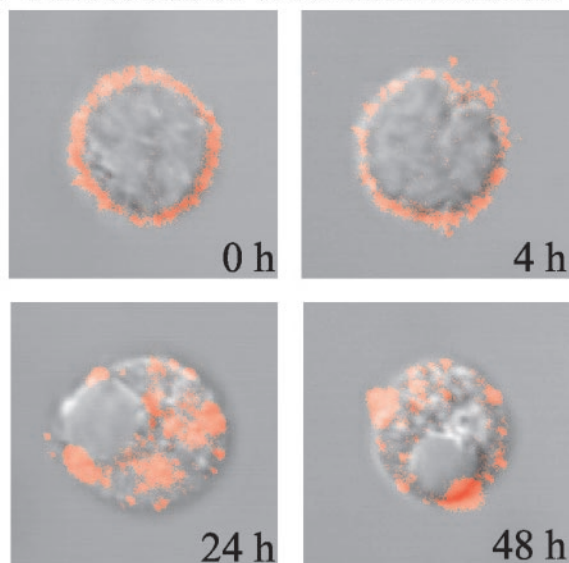
trol did not change for T-cells (control: 74%, $n = 1$; TA-2-treated: $70 \pm 2\%$, $n = 3$) but increased for B-cells (control: 12%, $n = 1$; TA-2-treated: $21 \pm 3\%$, $n = 3$). Since T- and B-cells are normally $\alpha_4\beta_1$ -positive but are devoid of surface $\alpha_4\beta_1$ following TA-2 treatment, these data provide evidence that this observed effect is not due to a loss of a lymphocyte subclass.

Internalization of $\alpha_4\beta_1$ Integrin/TA-2 Complex. To determine whether the $\alpha_4\beta_1$ integrin was being down-modulated and internalized or whether the integrin was shed from the cell surface following TA-2 treatment, we directly labeled TA-2 with the fluorescent tag, Alexa594, and used confocal microscopy to follow the disappearance of $\alpha_4\beta_1$ from the cell surface. Results from the study are shown in Fig. 8. First, we isolated splenocytes from an untreated Lewis rat, incubated them with TA-2 ex vivo for 0, 4, 24, and 48 h and monitored the arrangement of TA-2/ $\alpha_4\beta_1$ complexes by confocal microscopy. Figure 8A shows the time course of TA-2 binding and internalization in rat splenocytes. At 0 h, the fluorescently tagged TA-2 was uniformly bound to the cell surface with none appearing in the cell cytoplasm. At 4 h, the staining was less uniform with capping beginning to occur, represented by the patchy areas of fluorescence on the cell surface. By 24 and 48 h, the cell cytoplasm showed dense areas of internalized TA-2 with less fluorescence associated with cell surface. Because of the low density of $\alpha_4\beta_1$ on splenocytes, we were unable to observe a measurable fluorescent signal when they were treated with BIO8139-Alexa594. Consequently, we tested binding of BIO8139-Alexa594 to the RBL.1 rat cell line, which express a higher density of cell surface integrin. RBL.1 cells were treated with a saturating dose of BIO8139-Alexa594 or TA-2-Alexa594 for 30 min at 4°C then incubated for 0, 4, 24, or 48 h. The observed capping and internalization of TA-2 is shown (Fig. 8B) compared with BIO8139 (Fig. 8C) in RBL.1 cells at 0 and 48 h using confocal microscopy. At time 0, 30 min after the addition of the probes at 4°C, TA-2-Alexa594 or BIO8139-Alexa594 uniformly saturated the cell membrane whereas the cell cytoplasm was devoid of fluorescence (Fig. 8, B and C, 0 h). At 48 h, capping of the TA-2/ $\alpha_4\beta_1$ complex was striking on the cell surface (data not shown), and in most cells, the complex had internalized (Fig. 8B, 48 h). BIO8139 did not internalize and remained on the cell surface (Fig. 8C, 48 h).

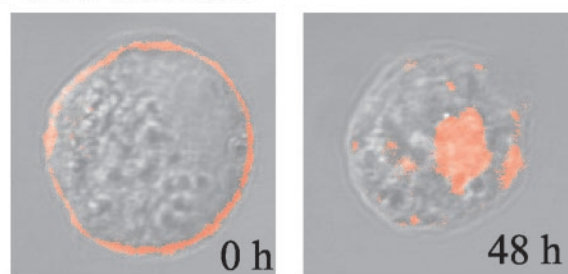
Discussion

We have investigated the role of $\alpha_4\beta_1$ in rat EAE using two types of inhibitors, an anti-rat α_4 monoclonal antibody TA-2, and the small molecule inhibitor BIO5192. Whereas both TA-2 and BIO5192 are potent inhibitors of $\alpha_4\beta_1$ and were efficacious in the EAE model, they are biochemically very different (see Table 2). The differences in their biochemical properties provided a means for understanding key features in the inhibition of $\alpha_4\beta_1$ function that lead to efficacy in EAE. First, the selectivity of BIO5192 for $\alpha_4\beta_1$ indicates that engagement of $\alpha_4\beta_1$ is a key event in the progression of the disease. Although TA-2 recognizes $\alpha_4\beta_1$ and $\alpha_4\beta_7$, from the BIO5192-selectivity data, we can infer that inhibition of $\alpha_4\beta_7$ is not necessary for efficacy in this rat EAE model. Second, although TA-2 treatment down-regulated $\alpha_4\beta_1$ expression, BIO5192 treatment had no effect on $\alpha_4\beta_1$ expression, indicating that blockade of $\alpha_4\beta_1$ is sufficient for inhibiting EAE.

A. Timecourse of TA-2 internalization



B. TA-2-Alexa594



C. BIO8139-Alexa594

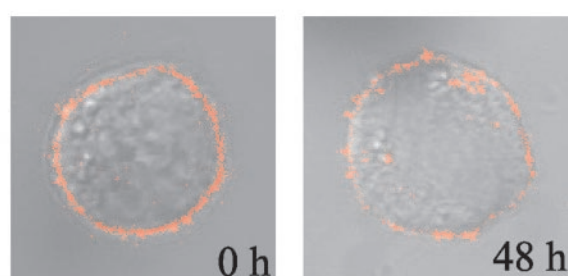


Fig. 8. Confocal imaging and internalization of the integrin $\alpha_4\beta_1$ receptor/TA-2 complex. Rat splenocytes were treated with TA-2 for 0, 4, 24, and 48 h (A) or RBL.1 cells treated with either TA-2-Alexa594 (B) or BIO8139-Alexa594 (C) for 0 and 48 h. Images were taken with a Leitz Plan-Apochromatic 63 \times (1.32 numerical aperture, oil immersion) objective (Leica) for the RBL.1 cells and 100 \times objective for the splenocytes, with a 2 \times digital zoom. Each frame represents a single optical section from the middle section of the cells observed for internalization under all conditions. The fluorescent images were overlaid onto Neumarski images of the cells. Note: there is no staining in the nucleus.

Other differences in the biochemical properties of TA-2 and BIO5192 include metal ion dependencies, valency, and LIBS binding. In particular since TA-2 contains two α_4 -binding sites and BIO5192 has only one, the difference in valency is likely to have led to the capping phenomenon observed with TA-2 and subsequent events leading to down modulation.

The observation that no cell surface $\alpha_4\beta_1$ remained after treatment with TA-2 was surprising since others have observed only a slight down-regulation (Bretscher, 1992; Sel-

TABLE 2

Comparative properties of BIO5192 and TA-2
Summary of the biochemical, PK, and PD properties of BIO5192 and TA-2 and their efficacy in rat EAE.

Properties	BIO5192	mAb TA-2
Selectivity	$\alpha_4\beta_1$	$\alpha_4\beta_1/\alpha_4\beta_7$
Species specificity	Human, mouse, rat, sheep, dog	Rat
Binds unactivated and activated $\alpha_4\beta_1$	+	+
Binding inhibition by EDTA	+	-
LIBS inducer	+	-
K_D	<10 pM	30 pM
Valency	Monovalent	Divalent
PK (i.v.) $t_{1/2}$	1.1 h	48 h
Lymphocytosis	+	+
Down modulates $\alpha_4\beta_1$	-	+
Clusters $\alpha_4\beta_1$	-	+
Efficacy in EAE	+	+

maj et al., 1998). The significance is unknown, but may reflect the contributions of other downstream effects on its binding. Several groups have reported downstream effects of blocking the $\alpha_4\beta_1$ /VCAM-1 interaction. Leussink et al. (2002) showed that inhibition of $\alpha_4\beta_1$ /VCAM-1 interactions by mAb TA-2 led to a decrease in cytokine production, including interferon- γ and TNF α , and induction of T-cell apoptosis in rat experimental autoimmune neuritis. Furthermore, when a TNF-binding protein was administered in a passive transfer model of mouse EAE, lower TNF levels caused a decrease in VCAM-1 expression in the central nervous system and a down-regulation of $\alpha_4\beta_1$ expression on splenocytes (Selmaj et al., 1998). In another study, treatment with anti- α_4 mAb 9C10 induced apoptosis of CD4 $^+$ and CD8 $^+$ T-cells resulting in activation of protein kinase C during T-cell development and following mature T-cell activation (Tchilian et al., 1997). To determine whether BIO5192 could elicit a signaling response, we performed a gene chip analysis on human THP1 cells with and without BIO5192 treatment (A. R. deFougerolles, R. B. Pepinsky, R. R. Lobb, V. E. Kotliansky, data not shown). As expected BIO5192, as a monomer, was unable to induce a signal. Although TA-2 treatment may be having a secondary effect in our studies, the data with BIO5192 indicate that in EAE this is not necessary for efficacy.

TA-2 and BIO5192 treatments both induced a lymphocytosis and were efficacious in the EAE model. To verify the relationship between lymphocytosis and efficacy, we tested several other $\alpha_4\beta_1$ inhibitors with distinct biochemical properties (data not shown). The small molecule $\alpha_4\beta_1$ inhibitor, (*R*)-*N*-[[4-[[[(2-methylphenylamino)-carbonyl]amino]phenyl]acetyl]-*L*-prolyl-3-methyl]- β -alanine, had an IC_{50} of 25 nM, did not elicit a lymphocytosis response, and was inactive in rat EAE. We also tested an inhibitor compound **3** (Pepinsky et al., 2002), which induced a very transient lymphocytosis due to a short serum half-life, which also failed in EAE. Although compound **3** was a low nanomolar inhibitor of the nonactivated integrin, it failed to maintain receptor occupancy following a 30 mg/kg s.c. dosing. We infer from these studies that a constant coverage of $\alpha_4\beta_1$ by the inhibitor is a prerequisite for lymphocytosis and for activity in EAE. Lymphocytosis is a simple pharmacodynamic marker for blockade of $\alpha_4\beta_1$ function and can be used as a surrogate marker for selecting dosing regimens. From our studies, it is unclear if the elevated cell number is due to the release of $\alpha_4\beta_1$ -positive

leukocytes from VCAM-1 expressed on blood vessel endothelial cells or stroma or a block of trafficking lymphocytes accompanied by their inability to leave the blood compartment. The speed of the effect following BIO5192 treatment best supports the displacement hypothesis.

The role of $\alpha_4\beta_7$ in EAE has been controversial. The $\alpha_4\beta_7$ /MAdCAM-1 pathway was shown to contribute to the EAE response in a nonremitting EAE model induced by myelin oligodendrocyte glycoprotein 35–55-stimulated T-cells (Kanwar et al., 2000a,b). Kanwar et al. showed that an anti-MAdCAM-1 antibody alone or in combination with anti-VCAM-1 and anti-intercellular adhesion molecule-1 induced remission of EAE, with combination therapy leading to a more rapid remission. Conversely, Engelhardt et al. (Engelhardt et al., 1995, 1998; Laschinger and Engelhardt, 2000) examined the roles of $\alpha_4\beta_1$ and $\alpha_4\beta_7$ in transfer and active models of EAE in mice using monoclonal antibodies to $\alpha_4\beta_1$, $\alpha_4\beta_7$, the β_7 -chain and VCAM-1 and demonstrated that $\alpha_4\beta_7$ integrin is not essential for the development of EAE. MAdCAM-1 was never detected on blood-brain barrier endothelial cells during EAE in SJL/J or C57Bl/6 mice. The BIO5192 studies presented here support this latter study demonstrating that inhibition of $\alpha_4\beta_7$ is not necessary. One explanation for these conflicting results is that MAdCAM-1 is interacting with $\alpha_4\beta_1$, and therefore the effect of the anti-MAdCAM-1 is not on inhibition of $\alpha_4\beta_7$ but was a direct effect on $\alpha_4\beta_1$ function. In support of this hypothesis, Newham et al. (1998) showed that MAdCAM-1 binds $\alpha_4\beta_1$. Also since $\alpha_4\beta_7$ binds to osteopontin (Bayless et al., 1998) in the brain, MAdCAM-1 may not be involved. Alternatively, the discrepancy may represent differences in the EAE model used by Kanwar et al. (2000a,b) and would require a more thorough evaluation.

Multiple sclerosis is characterized by lymphocytes that migrate and infiltrate into the central nervous system and brain affecting demyelination of nerve cells causing the disease (Miller et al., 2003). Various aspects of multiple sclerosis have been recapitulated in rodent models of EAE, with differing effects and efficacy profiles of $\alpha_4\beta_1$ inhibition observed in rats and mice (Kanwar et al., 2000a,b). Rat EAE is usually monophasic, and $\alpha_4\beta_1$ inhibition delays the onset of disease. Our results confirm and extend these original observations. Mouse EAE is usually relapsing/remitting characterized by epitope spreading and activated T-cell involvement. Engelhardt et al. confirmed in a mouse model of EAE that blockade of α_4 /VCAM-1 interaction was involved in inflammatory cell recruitment across the blood-brain barrier and that inhibition of $\alpha_4\beta_1$ -dependent adhesion of antigen-specific T-cells to blood-brain barrier endothelium was important for efficacy (Engelhardt et al., 1995, 1998; Laschinger and Engelhardt, 2000). In another model, PS/2, an anti-mouse α_4 antibody, inhibited EAE when administered prophylactically but exacerbated disease when given therapeutically in established disease (Theien et al., 2001). We saw no evidence of an exacerbation of disease when treatment was stopped in rats. Furthermore, in human clinical trials in which the anti- α_4 mAb natalizumab was administered to patients with relapsing/remitting multiple sclerosis, clinical benefits were observed while natalizumab maintained adequate serum levels, and disease activity returned to baseline when the drug was withdrawn. The exacerbation of disease seen in the relapsing mouse model was not seen in patients

during clinical trials (Miller et al., 2003) and may be specific for this mouse model.

Of the many small molecule inhibitors that have been developed from the LDV sequence of CS1, BIO5192 is the most potent and selective $\alpha_4\beta_1$ inhibitor developed to date (Abraham, 1997; Lin et al., 1999; Kudlacz et al., 2002; van der Laan et al., 2002). Lin et al. (1999) reported that BIO1211, $K_D = 70$ pM for Mn^{2+} -activated $\alpha_4\beta_1$, is efficacious in a sheep asthma model. BIO1211 is only a 20 to 40 nM inhibitor of nonactivated $\alpha_4\beta_1$ and therefore was not expected to be effective if the nonactivated $\alpha_4\beta_1$ was important for function. BIO1211 was inactive in EAE when administered at 30 mg/kg. A second compound, the CS1 ligand mimic, phenylacetyl-L-leucyl-L-aspartyl-L-phenylalanyl-D-prolineamide, was efficacious in the sheep asthma model and partially effective in active rat EAE (Abraham, 1997; van der Laan et al., 2002). A third compound, CP-664511, which is related to BIO1211, is a 5 nM $\alpha_4\beta_1$ inhibitor in serum and efficacious in an antigen-induced pulmonary eosinophil infiltration model. The extraordinary potency of BIO5192, <10 pM for activated and unactivated integrin and because it binds $\alpha_4\beta_1$ from many species, including mouse, rat, sheep, dog and humans, makes BIO5192 a particularly attractive compound for investigating $\alpha_4\beta_1$ function. In summary, we have compared the biochemical, pharmacological, and pharmacodynamic properties and efficacy in a rat model of EAE, of two $\alpha_4\beta_1$ inhibitors, mAb TA-2 and BIO5192. TA-2 provides a benchmark for assessing $\alpha_4\beta_1$ function in rats against which we tested the highly selective $\alpha_4\beta_1$ inhibitor BIO5192. Both inhibitors induced a lymphocytosis, a PD marker of activity, and were efficacious in EAE. Treatment with TA-2 caused a decrease in $\alpha_4\beta_1$ integrin expression on the cell surface, which resulted from internalization of the $\alpha_4\beta_1$ integrin/TA-2 complex. In contrast, BIO5192 did not modulate cell surface $\alpha_4\beta_1$, indicating that blockade of $\alpha_4\beta_1$ /ligand interactions is sufficient for function in EAE. The use of potent selective $\alpha_4\beta_1$ integrin inhibitors therapeutically for treatment of inflammatory diseases may be an important alternative to therapy when inhibition is the mechanism necessary to alter disease.

Acknowledgments

We thank Chris Ehrenfels for confocal instruction, Sukumori Mohan and Akos Szilvasi for performing FACS analysis, Martin Hemler and S. Burakoff for cell lines, members of the Biogen-Merck Joint Task Force for helpful discussions, and Shelia Violette for support of the manuscript.

References

- Abraham WM (1997) Blockade of late-phase airway responses and airway hyperresponsiveness in allergic sheep with a small-molecule peptide inhibitor of VLA-4. *Am J Respir Crit Care Med* **156**:696–703.
- Bayless KJ, Meininger GA, Scholtz JM, and Davis GE (1998) Osteopontin is a ligand for the $\alpha_4\beta_1$ integrin. *J Cell Sci* **111**:1165–1174.
- Bretscher M (1992) Circulating integrins: $\alpha_5\beta_1$, $\alpha_6\beta_4$ and Mac-1, but not $\alpha_3\beta_1$, $\alpha_4\beta_1$ or LFA-1. *EMBO J* **11**:405–410.
- Chen LL, Whitty A, Scott D, Lee WC, Cornebise M, Adams SP, Petter RC, Lobb RR, and Pepinsky RB (2001) Evidence that ligand and metal ion binding to integrin $\alpha_4\beta_1$ are regulated through a coupled equilibrium. *J Biol Chem* **276**:36520–36529.
- Clark EA and Brugge JS (1995) Integrins and signal transduction pathways: the road taken. *Science (Wash DC)* **268**:233–239.
- Enders U, Lobb R, Pepinsky RB, Hartung HP, Toyka KV, and Gold R (1998) The role of the very late antigen-4 and its counterligand vascular cell adhesion molecule-1 in the pathogenesis of experimental autoimmune neuritis of the Lewis rat. *Brain* **121**:1257–1266.
- Engelhardt B, Conley FK, Kilshaw PJ, and Butcher EC (1995) Lymphocytes infiltrating the CNS during inflammation display a distinctive phenotype and bind to VCAM-1 but not to MAdCAM-1. *Int Immunol* **7**:481–491.

- Engelhardt B, Laschinger M, Schulz M, Samulowitz U, Vestweber D, and Hoch G (1998) The development of experimental autoimmune encephalomyelitis in the mouse requires alpha4-integrin but not alpha4beta7-integrin. *J Clin Invest* **102**:2096–2105.
- Hojó M, Maghni K, Issekutz TB, and Martin JG (1998) Involvement of alpha-4 integrins in allergic airway responses and mast cell degranulation in vivo. *Am J Respir Crit Care Med* **158**:1127–1133.
- Humphries M (1996) Integrin activation: the link between ligand binding and signal transduction. *Curr Opin Cell Biol* **8**:632–640.
- Issekutz AC, Ayer L, Miyasaka M, and Issekutz TB (1996) Treatment of established adjuvant arthritis in rats with monoclonal antibody to CD18 and very late activation antigen-4 integrins suppresses neutrophil and T-lymphocyte migration to the joints and improves clinical disease. *Immunology* **88**:569–576.
- Issekutz TB (1991) Inhibition of in vivo lymphocyte migration to inflammation and homing to lymphoid tissues by the TA-2 monoclonal antibody. A likely role for VLA-4 in vivo. *J Immunol* **147**:4178–4184.
- Issekutz TB and Wykretowicz A (1991) Effect of a new monoclonal antibody, TA-2, that inhibits lymphocyte adherence to cytokine stimulated endothelium in the rat. *J Immunol* **147**:109–116.
- Kanwar JR, Harrison JE, Wang D, Leung E, Mueller W, Wagner N, and Krissansen GW (2000a) Beta7 integrins contribute to demyelinating disease of the central nervous system. *J Neuroimmunol* **103**:146–152.
- Kanwar JR, Kanwar RK, Wang D and Krissansen GW (2000b) Prevention of a chronic progressive form of experimental autoimmune encephalomyelitis by an antibody against mucosal addressin cell adhesion molecule-1, given early in the course of disease progression. *Immunol Cell Biol* **78**:641–645.
- Kudlacz E, Whitney C, Andresen C, Duplantier A, Beckius G, Chupak L, Klein A, Kraus K, and Milici A (2002) Pulmonary eosinophilia in a murine model of allergic inflammation is attenuated by small molecule antagonists. *J Pharmacol Exp Ther* **301**:747–752.
- Laschinger M and Engelhardt B (2000) Interaction of alpha4-integrin with VCAM-1 is involved in adhesion of encephalitogenic T cell blasts to brain endothelium but not in their transendothelial migration in vitro. *J Neuroimmunol* **102**:32–43.
- Leussink VI, Zettl UK, Jander S, Pepinsky RB, Lobb RR, Stoll G, Toyka KV, and Gold R (2002) Blockade of signaling via the very late antigen (VLA-4) and its counterligand vascular cell adhesion molecule-1 (VCAM-1) causes increased T cell apoptosis in experimental autoimmune neuritis. *Acta Neuropathol (Berl)* **103**:131–136.
- Lin K, Ateeq HS, Hsiung SH, Chong LT, Zimmerman CN, Castro A, Lee WC, Hammond CE, Kalkunte S, Chen LL, et al. (1999) Selective, tight-binding inhibitors of integrin alpha4beta1 that inhibit allergic airway responses. *J Med Chem* **42**:920–934.
- Lobb RR, Antognetti G, Pepinsky RB, Burkly LC, Leone DR, and Whitty A (1995) A direct binding assay for the vascular cell adhesion molecule-1 (VCAM1) interaction with alpha 4 integrins. *Cell Adhes Commun* **3**:385–397.
- Lobb RR and Hemler ME (1994) The pathophysiologic role of alpha 4 integrins in vivo. *J Clin Invest* **94**:1722–1728.
- Miller D, Khan O, Sheremata W, Blumhardt L, Rice G, Libonati M, Wilmer-Hulme A, Dalton C, Miszkiel K, O'Connor P and Group (2003) aINMST A controlled trial of natalizumab for relapsing multiple sclerosis. *N Engl J Med* **348**:15–23.
- Molossi S, Elices M, Arrhenius T, and Rabinovitch M (1995) Lymphocyte transendothelial migration toward smooth muscle cells in interleukin-1 beta-stimulated co-cultures is related to fibronectin interactions with alpha 4beta1 and alpha5beta1 integrins. *J Cell Physiol* **164**:620–633.
- Newham P, Craig SE, Clark K, Mould AP, and Humphries MJ (1998) Analysis of ligand-induced and ligand-attenuated epitopes on the leukocyte integrin alpha4beta1: VCAM-1, mucosal addressin cell adhesion molecule-1 and fibronectin induce distinct conformational changes. *J Immunol* **160**:4508–4517.
- Osborn L, Hession C, Tizard R, Vassallo C, Luhowskyj S, Chi-Rosso G, and Lobb R (1989) Direct expression cloning of vascular cell adhesion molecule 1, a cytokine-induced endothelial protein that binds to lymphocytes. *Cell* **59**:1203–1211.
- Pepinsky RB, Mumford RA, Chen LL, Leone D, Amo SE, Riper GV, Whitty A, Dolinski B, Lobb RR, Dean DC, et al. (2002) Comparative assessment of the ligand and metal ion binding properties of integrins alpha9beta1 and alpha4beta1. *Biochemistry* **41**:7125–7141.
- Ramos-Barbon D, Suzuki M, Taha R, Molet S, Issekutz TB, Hamid Q, and Martin JG (2001) Effect of alpha4-integrin blockade on CD4+ cell-driven late airway responses in the rat. *Am J Respir Crit Care Med* **163**:101–108.
- Schneider T, Issekutz TB, and Issekutz AC (1999) The role of alpha4 (CD49d) and beta2 (CD18) integrins in eosinophil and neutrophil migration to allergic lung inflammation in the Brown Norway rat. *Am J Respir Cell Mol Biol* **20**:448–457.
- Selmaj K, Walczak A, Mycko M, Berkowicz T, Kohno T, and Raine CS (1998) Suppression of experimental autoimmune encephalomyelitis with a TNF binding protein (TNFbp) correlates with down-regulation of VCAM-1/VLA-4. *Eur J Immunol* **28**:2035–2044.
- Takahashi H, Isobe T, Horibe S, Takagi J, Yokosaki Y, Sheppard D, and Saito Y (2000) Tissue transglutaminase, coagulation factor XIII and the pro-polypeptide of von Willebrand factor are all ligands for the integrins alpha9beta1 and alpha4beta1. *J Biol Chem* **275**:23589–23595.
- Taylor BM, Kolbasa KP, Chin JE, Richards IM, Fleming WE, Griffin RL, Fidler SF, and Sun FF (1997) Roles of adhesion molecules ICAM-1 and alpha4 integrin in antigen-induced changes in microvascular permeability associated with lung inflammation in sensitized Brown Norway rats. *Am J Respir Cell Mol Biol* **17**:757–766.
- Tchilian EZ, Owen JJ, and Jenkinson EJ (1997) Anti-alpha4 integrin antibody induces apoptosis in murine thymocytes and staphylococcal enterotoxin B-activated lymph node T cells. *Immunology* **92**:321–327.
- Theien BE, Vanderlugt CL, Eagar TN, Nickerson-Nutter C, Nazareno R, Kuchroo VK, and Miller SD (2001) Discordant effects of anti-VLA-4 treatment before and after onset of relapsing experimental autoimmune encephalomyelitis. *J Clin Invest* **107**:995–1006.
- van der Laan LJ, van der Goes A, Wauben MH, Ruuls SR, Dopp EA, De Groot CJ, Kuijpers TW, Elices MJ, and Dijkstra CD (2002) Beneficial effect of modified peptide inhibitor of alpha4 integrins on experimental allergic encephalomyelitis in Lewis rats. *J Neurosci Res* **67**:191–199.
- Wang JH, Pepinsky RB, Stehle T, Liu JH, Karpusas M, Browning B, and Osborn L (1995) The crystal structure of an N-terminal two-domain fragment of vascular cell adhesion molecule 1 (VCAM-1): a cyclic peptide based on the domain 1 C-D loop can inhibit VCAM-1-alpha 4 integrin interaction. *Proc Natl Acad Sci USA* **92**:5714–5718.
- Wayner EA, Garcia-Pardo A, Humphries MJ, McDonald JA, and Carter WG (1989) Identification and characterization of the T lymphocyte adhesion receptor for an alternative cell attachment domain (CS-1) in plasma fibronectin. *J Cell Biol* **109**:1321–1330.
- Wayner EA and Kovach NL (1992) Activation-dependent recognition by hematopoietic cells of the LDV sequence in the V region of fibronectin. *J Cell Biol* **116**:489–497.
- Yednock TA, Cannon C, Fritz LC, Sanchez-Madrid F, Steinman L, and Karin N (1992) Prevention of experimental autoimmune encephalomyelitis by antibodies against alpha 4 beta 1 integrin. *Nature (Lond)* **356**:63–66.

Address correspondence to: Diane R. Leone, Biogen, Inc., 12 Cambridge Center, Cambridge, MA 02142. E-mail: diane_leone@Biogen.com
